

An introduction to quantum Monte Carlo (for neutrino-nucleus scattering)

Alessandro Lovato

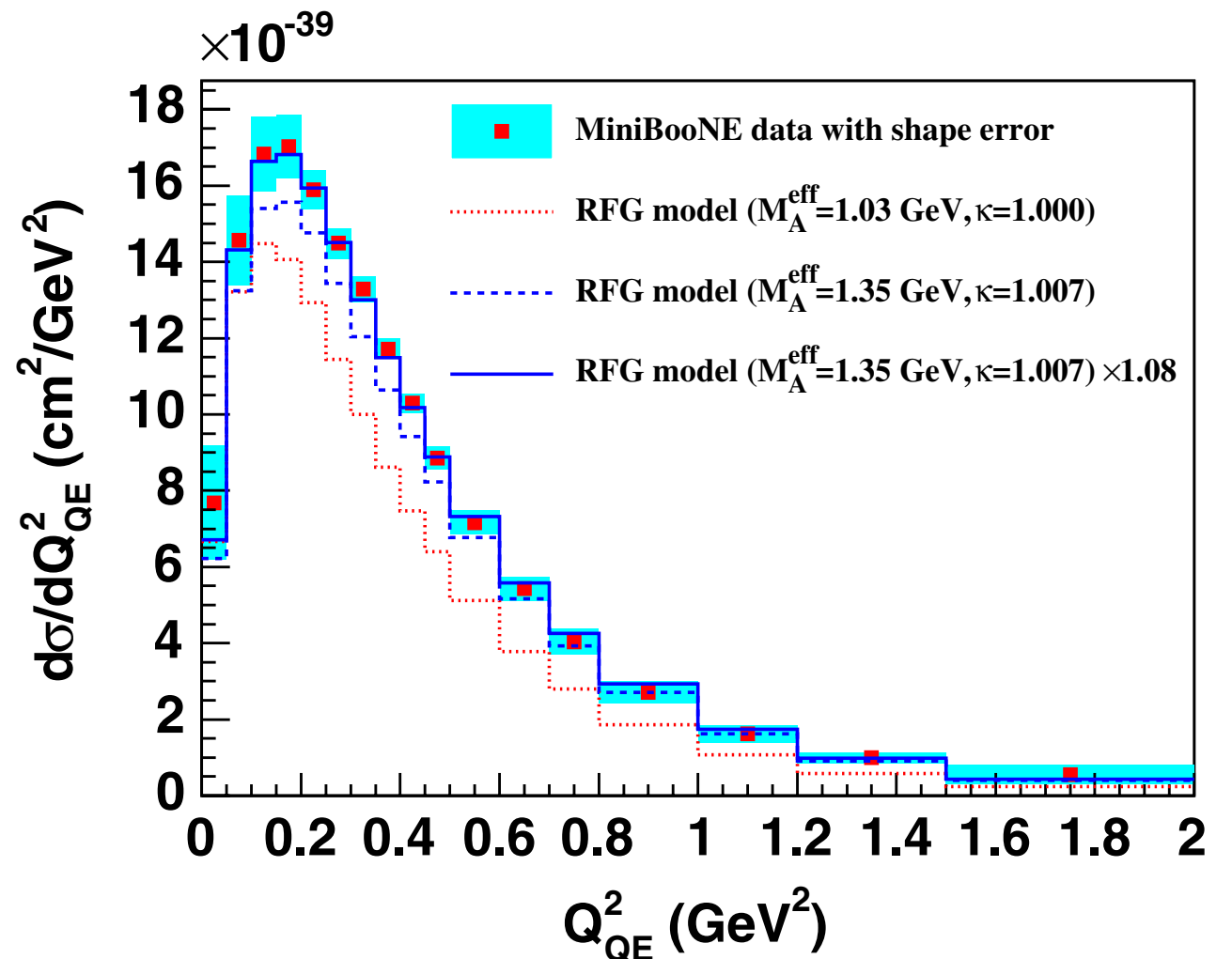


Chapter 1

Introduction

Why quantum Monte Carlo? (I)

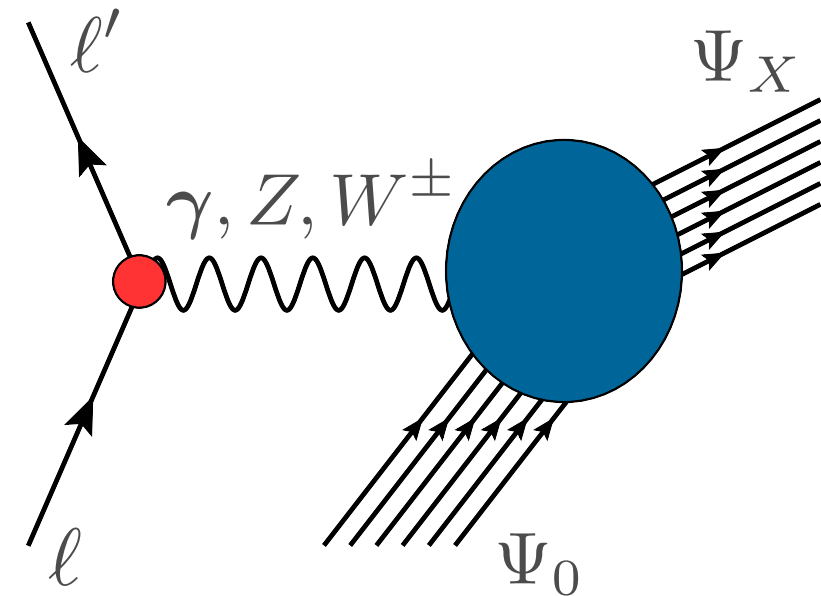
- The Relativistic Fermi gas model is not adequate to account for both the complexity of nuclear dynamics and the variety of reaction mechanisms contributing to the observed neutrino - nucleus cross section
- Quantum Monte Carlo (QMC) can be exploited to compute the electroweak response fully taking into account the correlations induced by the nuclear interactions and meson-exchange currents
- Neutrino experimental communities need accurate theoretical calculations, with reliable error estimates
- QMC methods allow for solving the time-independent Schrödinger equation for nuclear Hamiltonians and naturally provide estimates of the gaussian error of the calculation.



Lepton-nucleus scattering

The inclusive cross section of the process in which a lepton scatters off a nucleus and the hadronic final state is undetected can be written as

$$\frac{d^2\sigma}{d\Omega_\ell dE_{\ell'}} = L_{\mu\nu} W^{\mu\nu}$$



- The leptonic tensor $L_{\mu\nu}$ is fully specified by the lepton kinematic variables. For instance, in the electron-nucleus scattering case

$$L_{\mu\nu}^{\text{EM}} = 2[k_\mu k'_\nu + k_\nu k'_\mu - g_{\mu\nu}(kk')]$$

- The Hadronic tensor contains all the information on target response

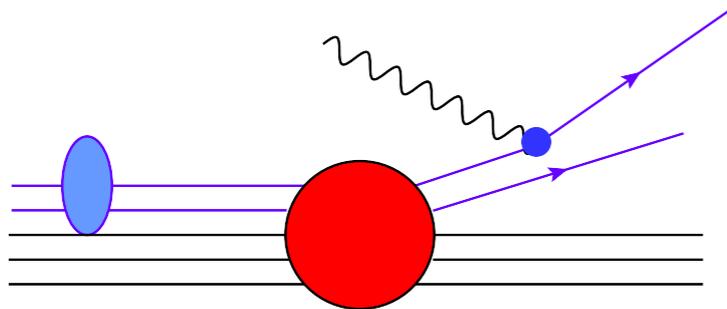
$$W^{\mu\nu} = \sum_X \langle \Psi_0 | J^{\mu\dagger}(q) | \Psi_X \rangle \langle \Psi_X | J^\nu(q) | \Psi_0 \rangle \delta^{(4)}(p_0 + q - p_X)$$

Note that the initial state does not depend on the momentum transfer!

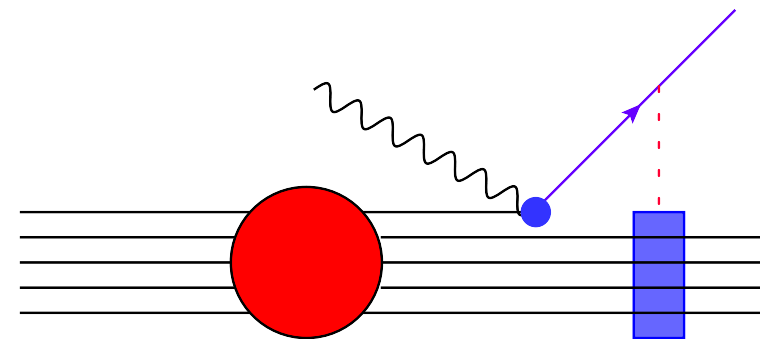
Two-body currents and nuclear correlations

Two-body meson exchange currents and nuclear correlations need to be fully accounted for in ab initio calculations of response functions

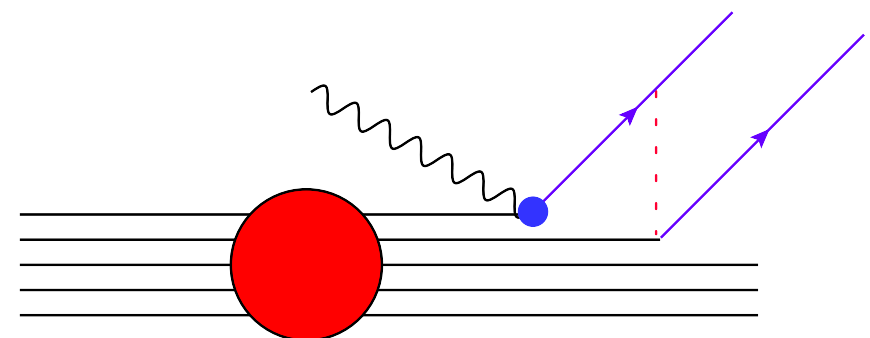
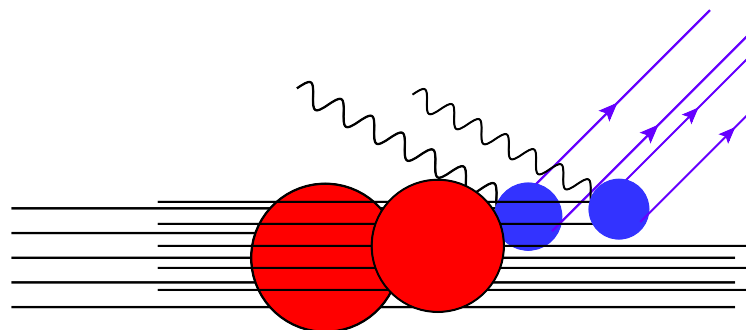
- Initial State Correlations



- Final State Interactions



- Meson Exchange Currents



Non-relativistic regime

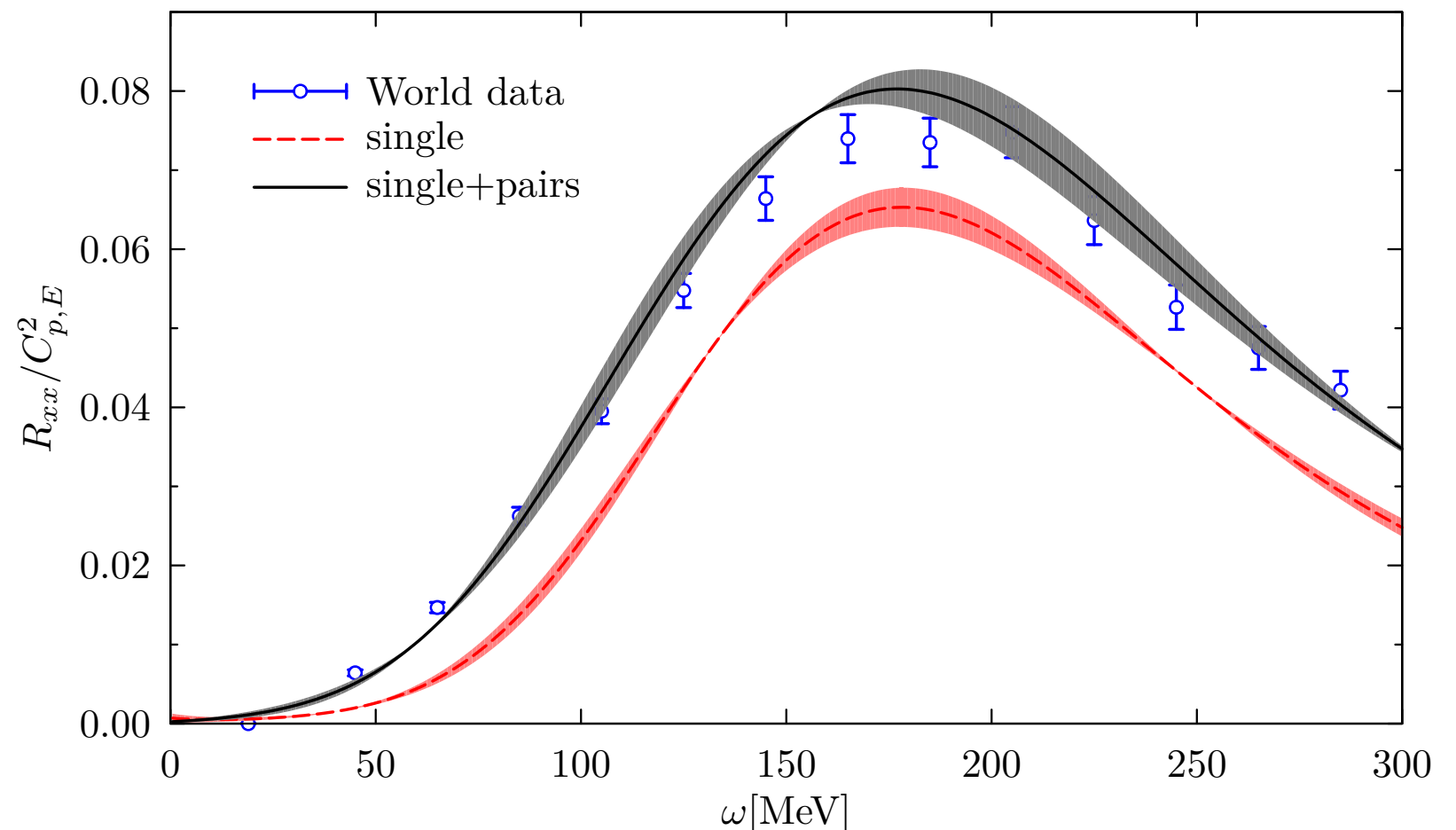
In the non-relativistic regime, typically corresponding to $|\mathbf{q}| \lesssim 500$ MeV, both the initial and the final state of the hadronic tensor are eigenstates of the nonrelativistic nuclear hamiltonian

$$H|\Psi_0\rangle = E_0|\Psi_0\rangle \quad H|\Psi_X\rangle = E_X|\Psi_X\rangle$$

As for the electron scattering on ^{12}C

$$|\Psi_X\rangle = |^{11}\text{B}, p\rangle, |^{11}\text{C}, n\rangle, |^{10}\text{B}, pn\rangle, |^{10}\text{B}, pp\rangle \dots$$

QMC calculation of the nuclear response from threshold up to the quasielastic region (for nuclei as large as ^{12}C) are currently carried out on leadership-class computers



Why quantum Monte Carlo? (II)

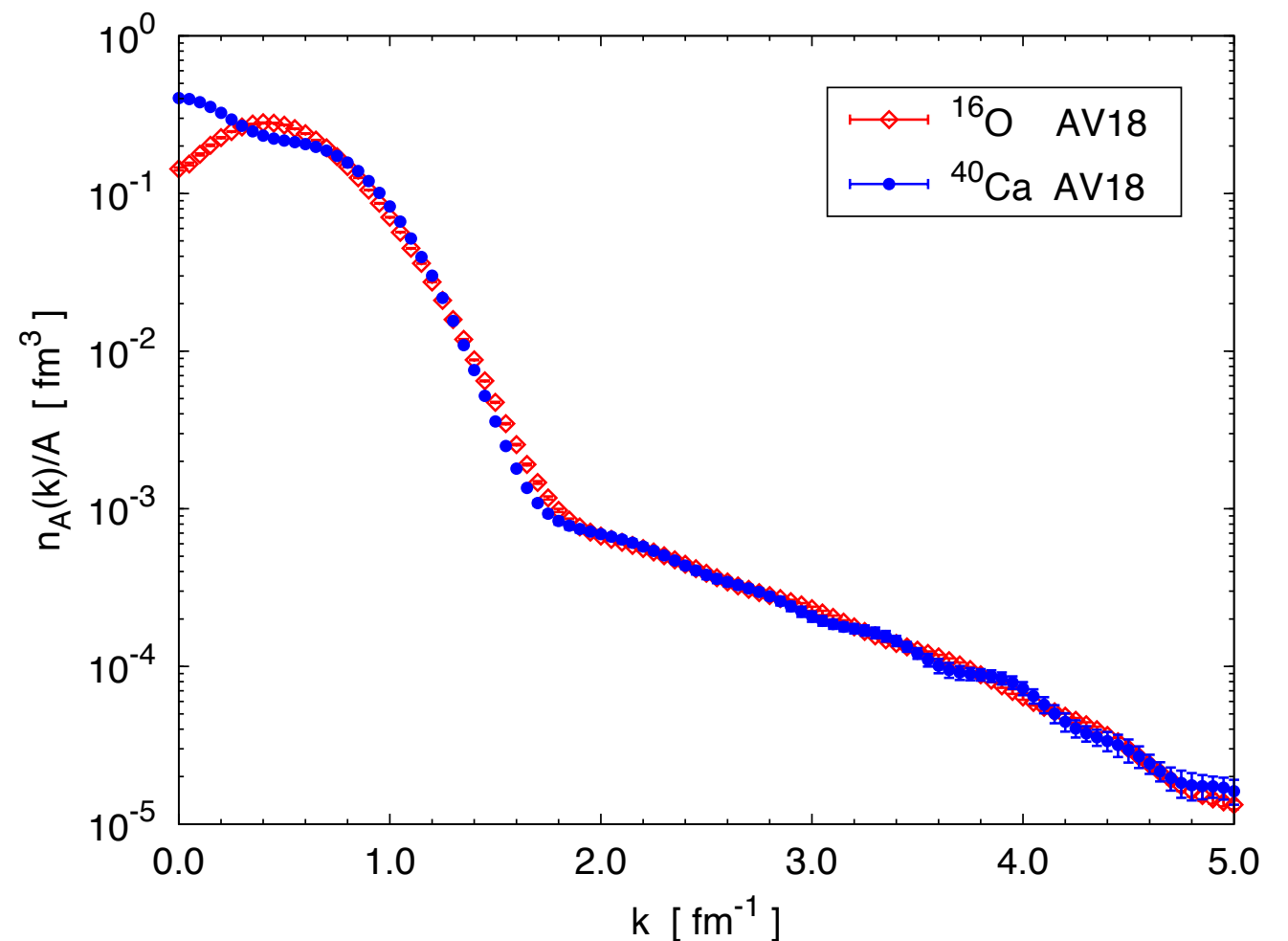
In the relativistic regime, the final state includes at least one particle carrying large momentum, whereas the initial nuclear state is still an eigenstate of the nuclear Hamiltonian.

The spectral function formalism allow one to circumvent the difficulties associated with the relativistic treatment of the nuclear final state and current operator, while at the same time preserving essential features (such as correlations) inherent to the realistic description of nuclear dynamics

The sum rule of the spectral function corresponds to the momentum distribution

$$\int dE P(\mathbf{k}, E) = n(\mathbf{k})$$

The momentum distribution of nuclei as large as ^{16}O and ^{40}Ca has been computed using QMC fully accounting for the correlations of the nuclear ground state



Chapter 2

Nuclear potentials and currents

The nuclear Hamiltonian

In both the non-relativistic and relativistic regimes, the the protons and the neutrons of the initial nuclear state can be treated as point like non relativistic particles, the dynamics of which are described by the hamiltonian

$$H = \sum_i \frac{\mathbf{p}_i^2}{2m} + \sum_{i < j} v_{ij} + \sum_{i < j < k} V_{ijk} + \dots$$

The two-body potential is the most studied of all, with thousands of experimental NN scattering data points at laboratory energies from essentially zero to hundreds of MeV

Warning: non *ab initio* approaches DO NOT rely on the thousands NN scattering data

Attempts are now being made to understand NN interaction directly through lattice QCD, though much more development will be required before it can be used directly in studies of nuclei

In the last two decades, advances have been made using chiral effective field theory, which employs chiral symmetry and a set of low-energy constants to fit the NN scattering data.

Three-nucleon (3N) interactions effectively include the lowest nucleon excitation, the $\Delta(1232)$ resonance, and other nuclear effects



Two-body potential

The Argonne v_{18} is a finite, local, configuration-space potential controlled by ~4300 np and pp scattering data below 350 MeV of the Nijmegen database

It is expressed as a sum of electromagnetic and one-pion-exchange terms and phenomenological intermediate- and short-range parts, which can be written as an overall operator sum

$$v_{18}(r_{ij}) = v_{ij}^{\gamma} + v_{ij}^{\pi} + v_{ij}^I + v_{ij}^S = \sum_{p=1}^{18} v^p(r_{ij}) O_{ij}^p$$

- Static part $O_{ij}^{p=1-6} = (1, \sigma_{ij}, S_{ij}) \otimes (1, \tau_{ij})$ Deuteron, S- and D- wave phase shifts
- Spin-orbit $O_{ij}^{p=7-8} = \mathbf{L}_{ij} \cdot \mathbf{S}_{ij} \otimes (1, \tau_{ij})$ P-wave phase shifts

The remaining operators, including quadratic spin-orbit interaction and charge symmetry breaking effects, are needed to achieve the description of the Nijmegen scattering data with $\chi^2 \simeq 1$.

The Argonne v_{18} model has a total of 42 independent parameters. While the fit was made up to 350 MeV, the phase shifts are qualitatively good up to much larger energies ≥ 600 MeV

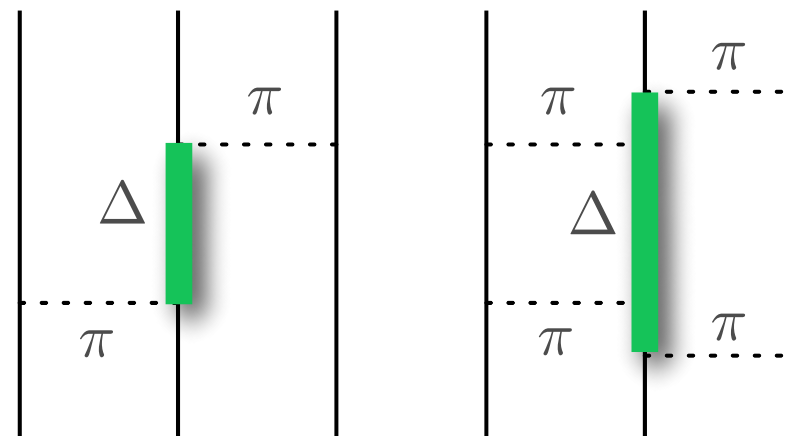
Three-body potential

An Hamiltonian which only includes Argonne v_{18} does not provide enough binding in the light nuclei and overestimates the equilibrium density of symmetric nuclear matter.

Three-body force is needed

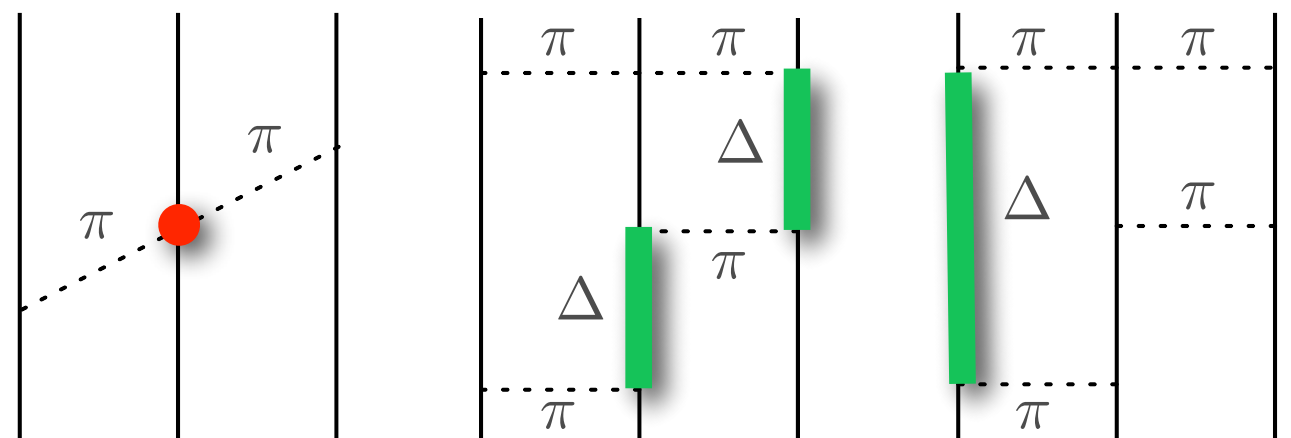
Urbana IX

contains the attractive Fujita and Miyazawa two-pion exchange interaction and a phenomenological repulsive term.



Illinois 7

also includes terms originating from three-pion exchange diagrams and the two-pion S-wave contribution.

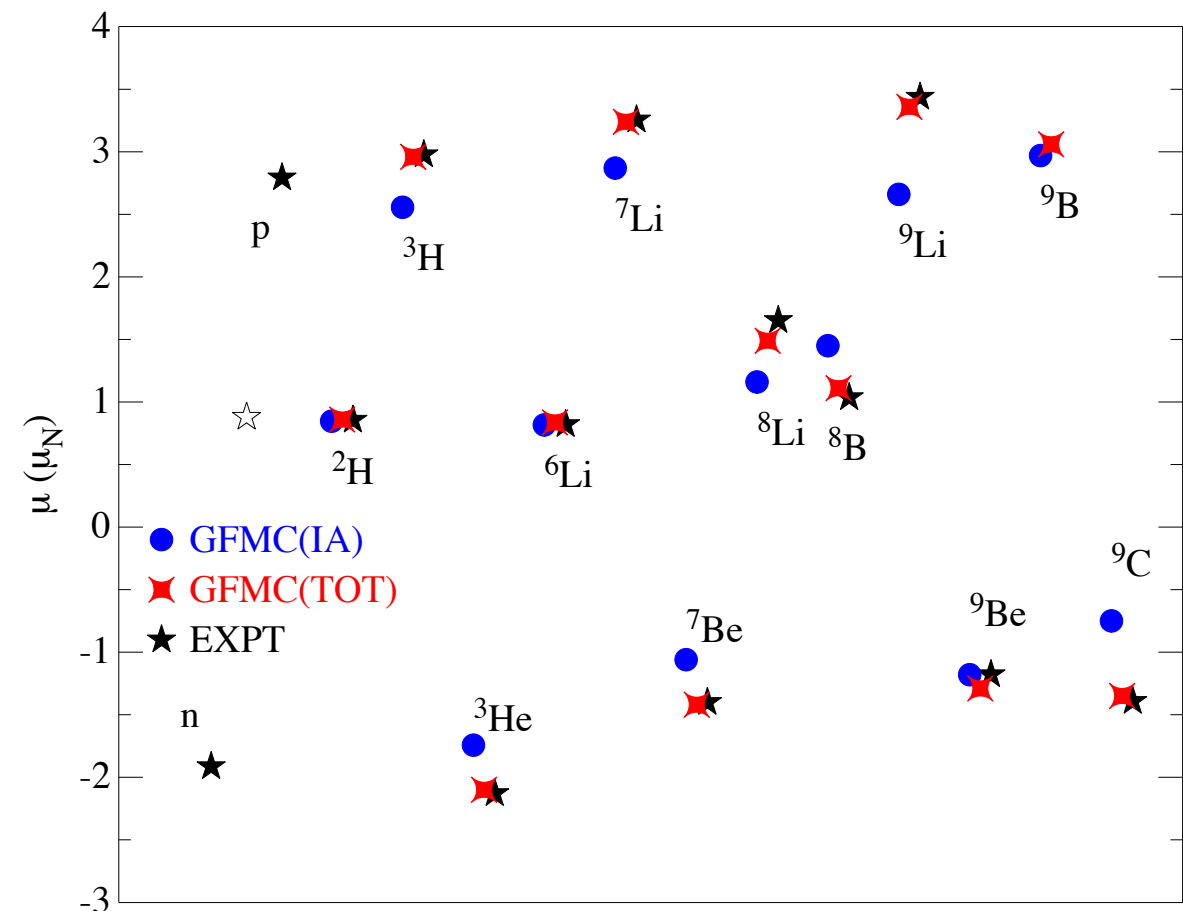
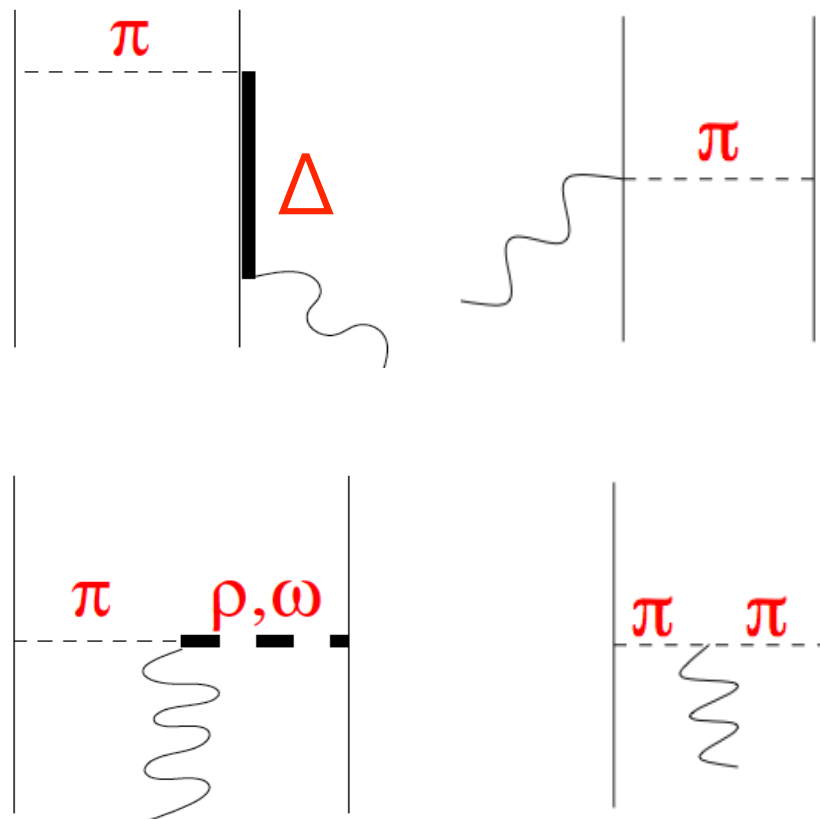


Nuclear currents

The nuclear electromagnetic current is constrained by the Hamiltonian through the continuity equation

$$\nabla \cdot \mathbf{J}_{\text{EM}} + i[H, J_{\text{EM}}^0] = 0$$

- Because the NN potential does not commute with the charge operator, the above equation implies that \mathbf{J}_{EM} involves two-nucleon contributions. They account for processes in which the vector boson couples to the currents arising from meson exchange between two interacting nucleons.
- The inclusion of two-body currents is essential for low-momentum and low-energy transfer transitions.



Chiral EFT

Chiral effective field theory (χ EFT) has witnessed much progress during the two decades since the pioneering papers by Weinberg (1990, 1991, 1992)

In χ EFT, the symmetries of quantum chromodynamics (QCD), in particular its approximate chiral symmetry, are employed to systematically constrain classes of Lagrangians describing the interactions of baryons with pions as well as the interactions of these hadrons with electroweak fields

Each class is characterized by a given power of the pion mass and/or momentum, the latter generically denoted by p , and can therefore be thought of as a term in a series expansion in powers of p/Λ_χ , where $\Lambda_\chi \simeq 1$ GeV specifies the chiral-symmetry breaking scale

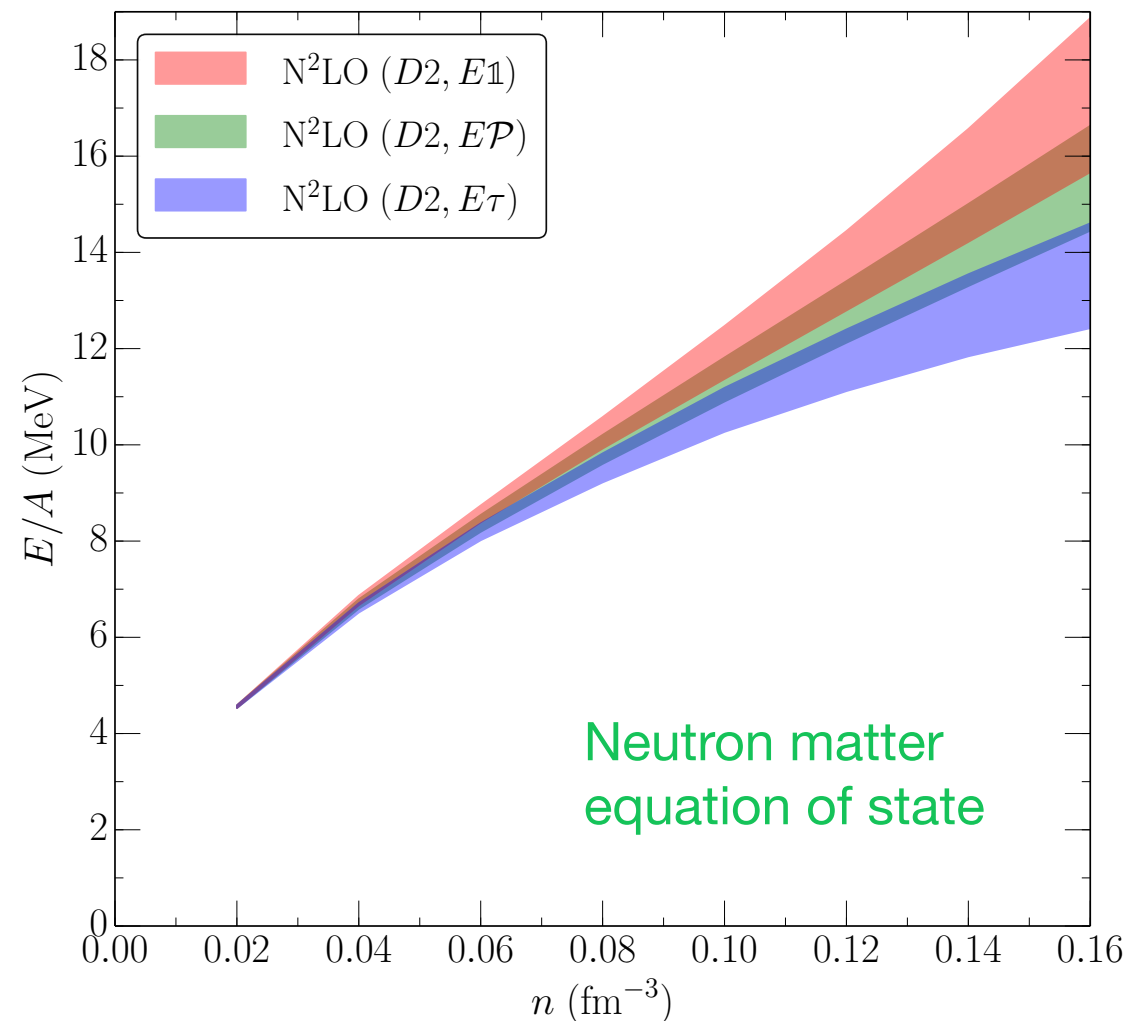
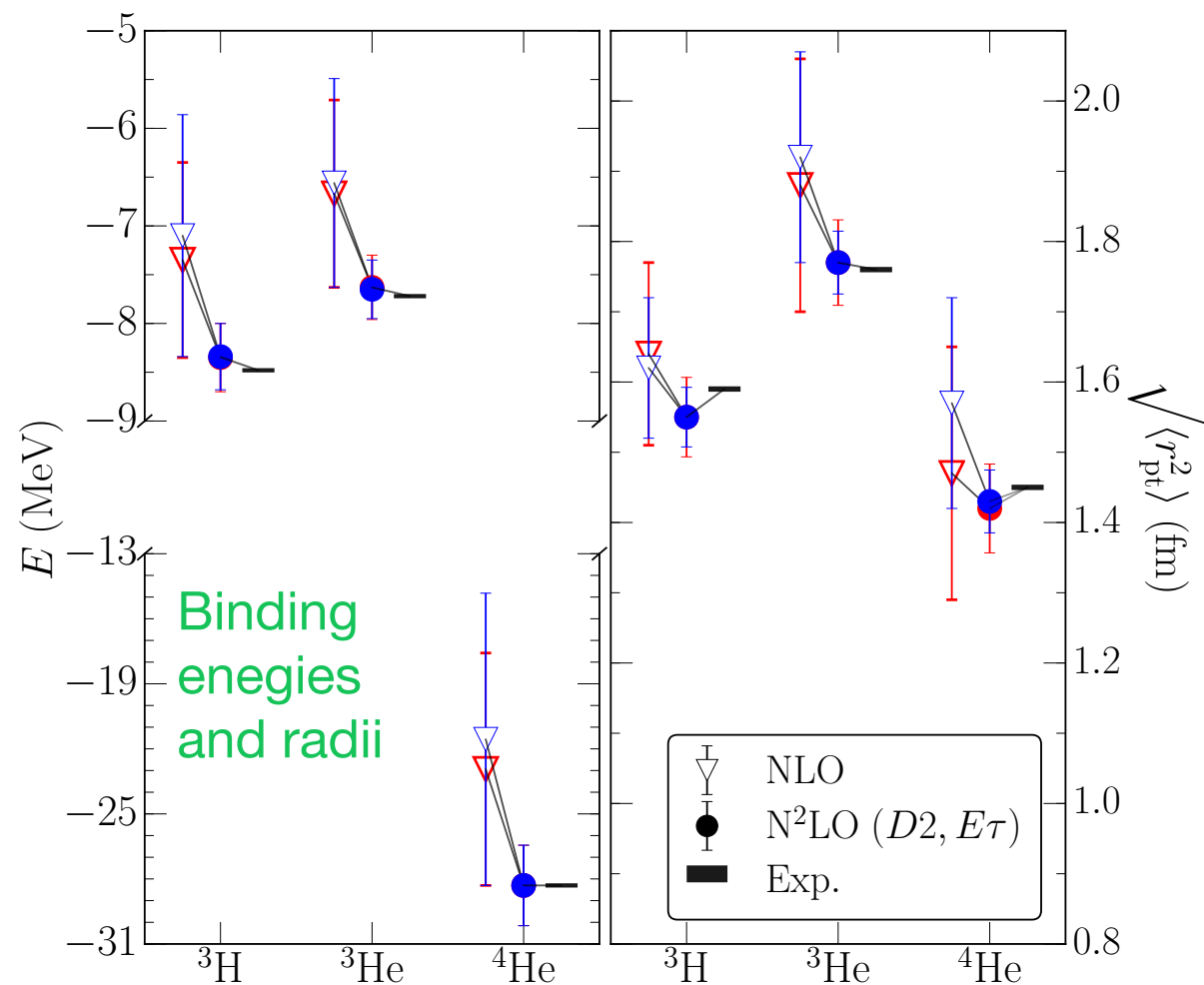
Each class also involves a certain number of unknown coefficients, called low-energy constants (LEC's), which are determined by fits to experimental data

Until very recently, nuclear potentials derived within χ EFT were highly non local. As a consequence, implementing them in quantum Monte Carlo was not feasible

Chiral EFT

Recently chiral nuclear interactions have been developed that are local up to next-to-next-to-leading order (N²LO). These interactions employ a different regularization scheme from previous chiral interactions, with a cutoff in the relative NN momentum.

They are therefore fairly simple to treat with standard QMC techniques to calculate properties of nuclei and neutron matter,



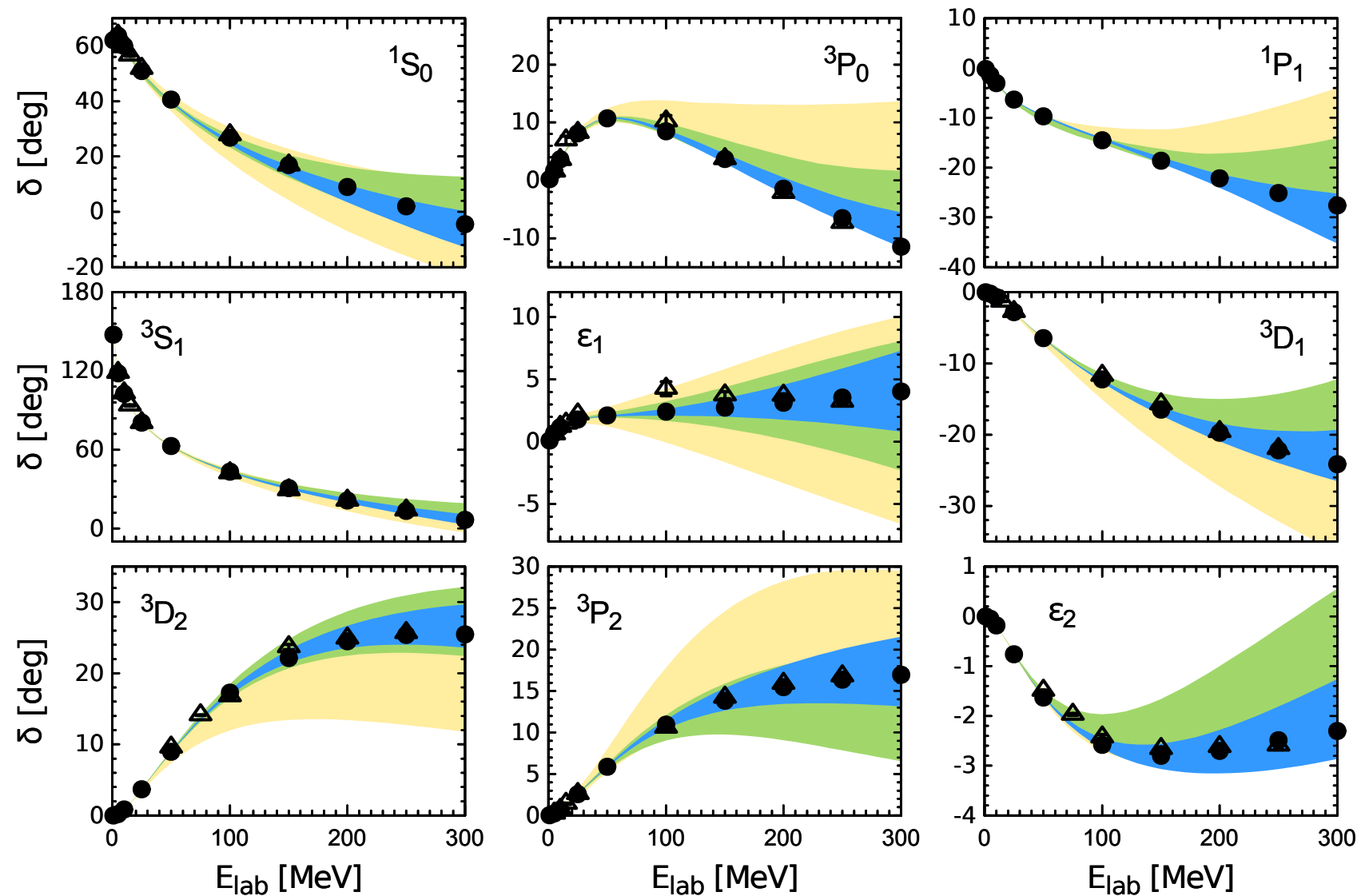
Chiral EFT

Within χ EFT nuclear potentials and currents obey a power counting scheme

	NN potential	NNN potential	NNNN potential
LO			
NLO			
N ² LO			
N ³ LO			

Chiral EFT

χ EFT provides a framework to derive consistent many-body forces and currents and the tools to rigorously estimate their uncertainties, along with a systematic prescription for reducing them

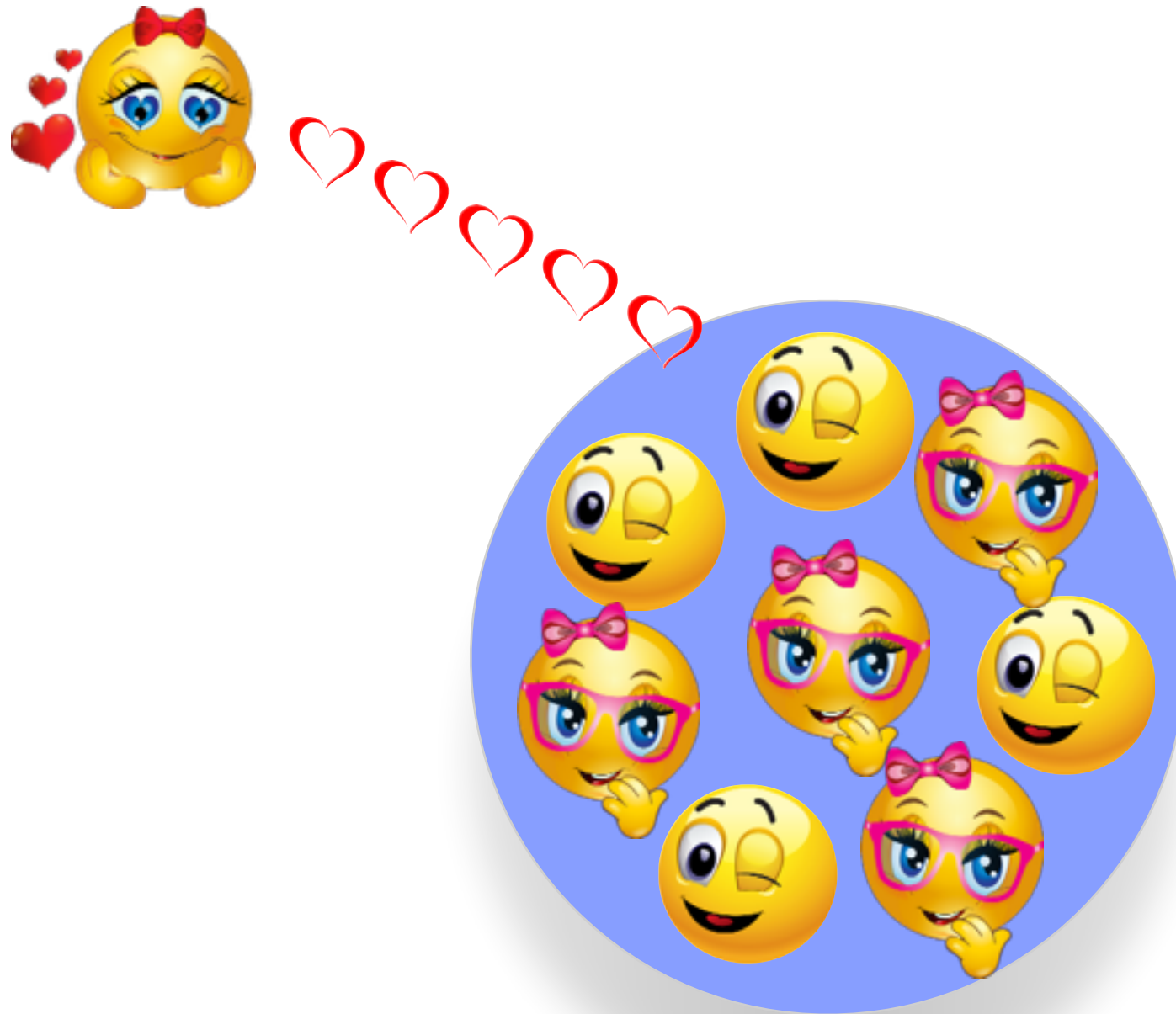


QMC is the only method allowing to disentangle the theoretical uncertainty arising from the nuclear interaction from the one associated with the many-body computational scheme.

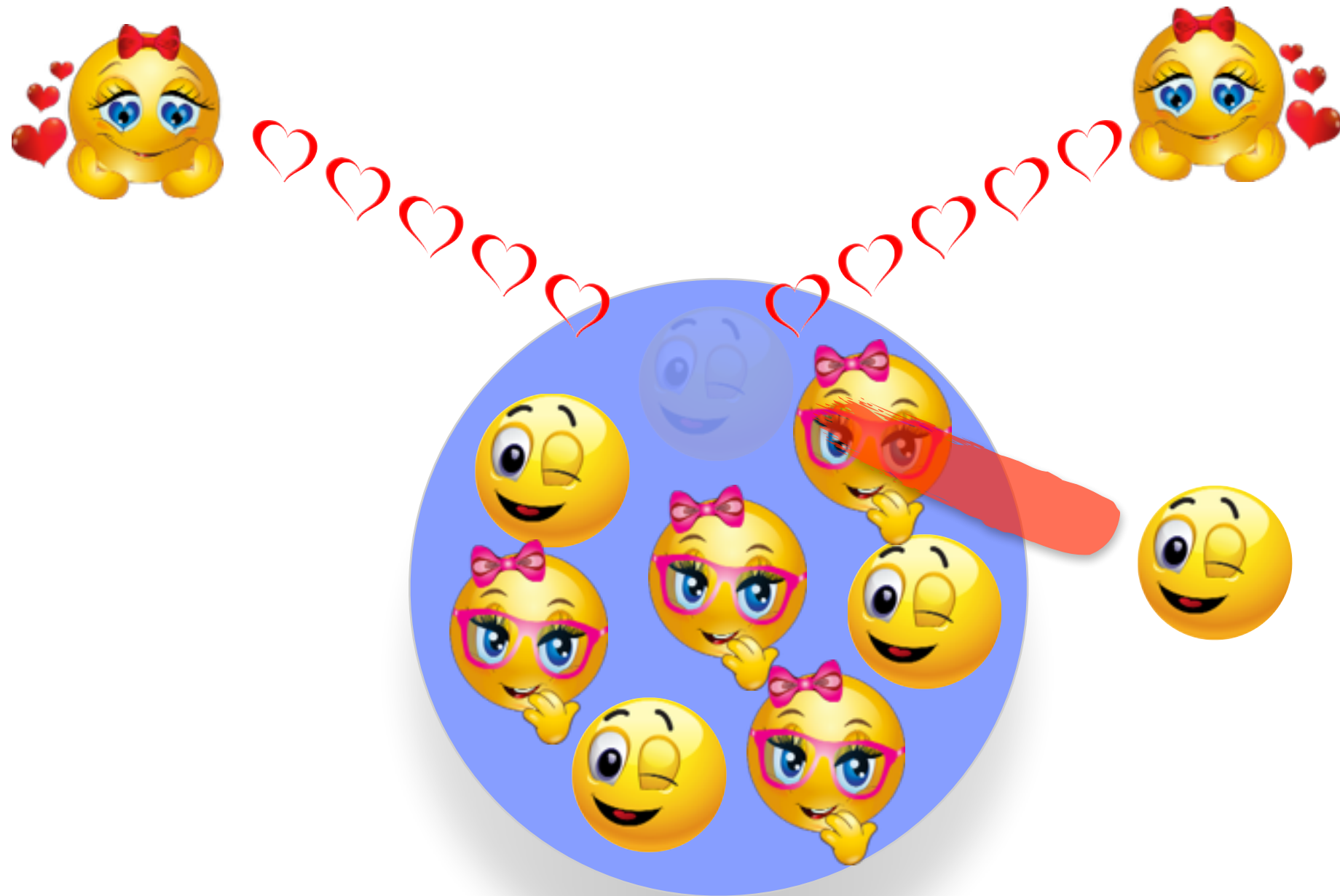
Chapter 2 bis

More on nuclear currents and correlations

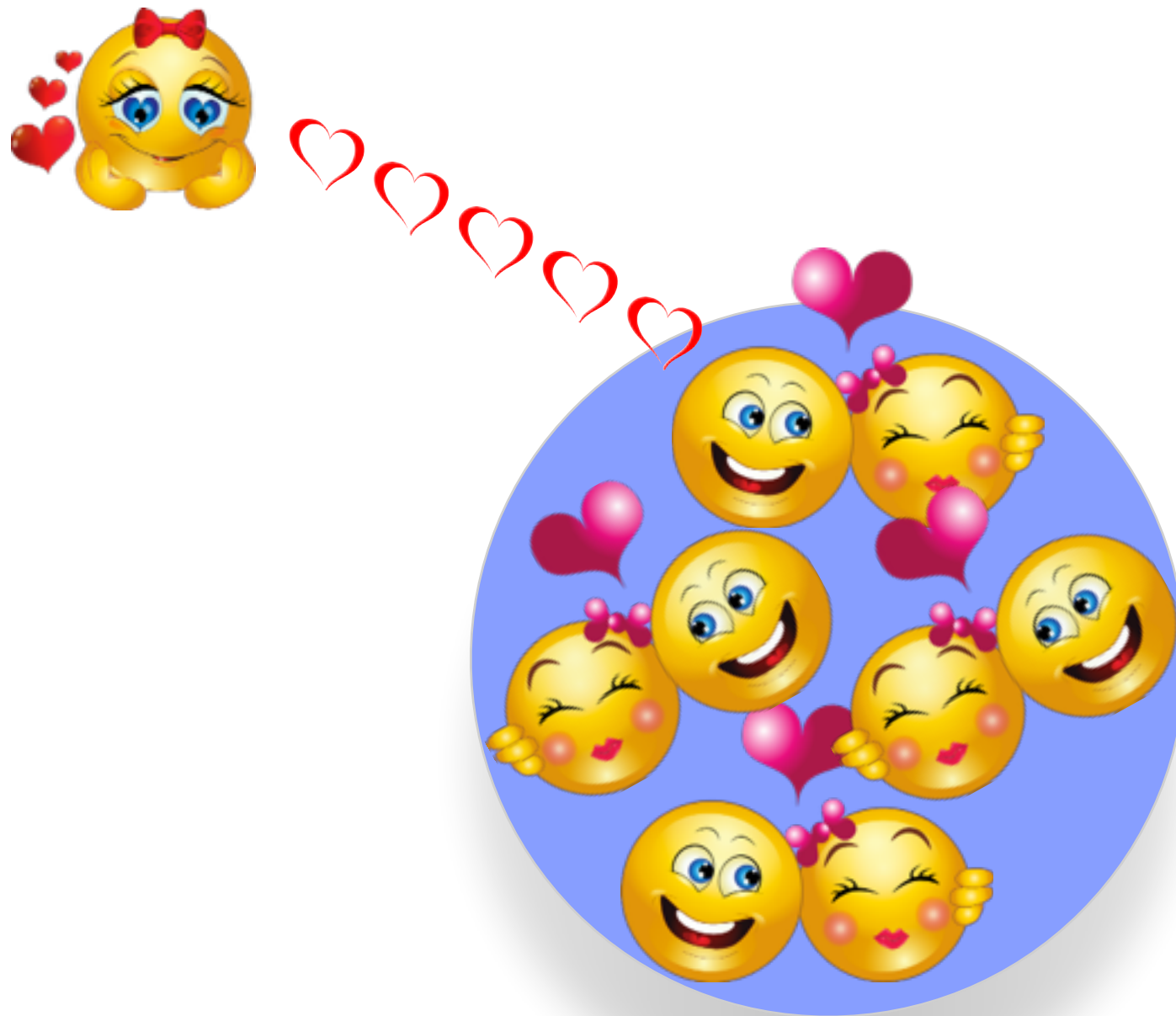
Scattering off uncorrelated nucleons



Scattering off uncorrelated nucleons



Scattering off correlated nucleons



Scattering off correlated nucleons



Scattering off correlated nucleons



Scattering off correlated nucleons



Chapter 3

An overview on quantum Monte Carlo

Why Quantum Monte Carlo? (III)

Quantum Monte Carlo provides us a way to go **from**

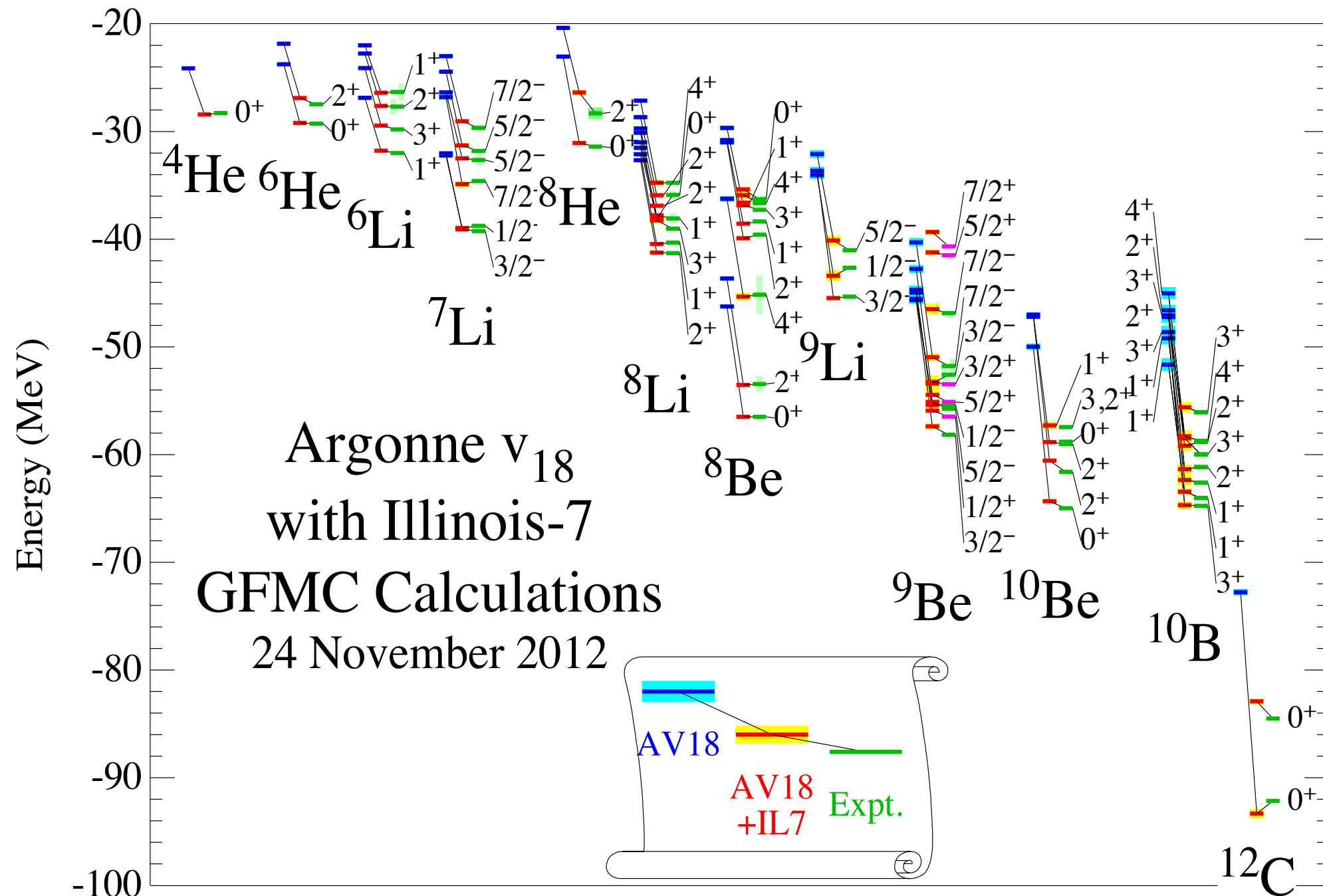
$$H = \sum_i \frac{\mathbf{p}_i^2}{2m} + \sum_{i < j} v_{ij} + \sum_{i < j < k} V_{ijk} + \dots$$

$$H|\Psi_0\rangle = E_0|\Psi_0\rangle$$



Why Quantum Monte Carlo? (III)

to... and more...



Quantum Monte Carlo methods

Let us assume that

- The temperature of the system is much smaller than the Fermi energy
- We are interested in the ground-state properties of the system

Quantum Monte Carlo methods give us two options for solving the many-body Schrödinger equation

Variational Monte Carlo (VMC)

In VMC, one assumes a form for the trial wave function and optimizes its variational parameters, typically by minimizing the energy and/or the variance of the energy. The expectation of the Hamiltonian is evaluated by means of Monte Carlo method.

Diffusion Monte Carlo (DMC)

“Exactly” solve the problem by projecting the ground state from an arbitrary initial guess of the wave function by means of a propagation in imaginary time.

Chapter 3

Variational Monte Carlo

Variational Monte Carlo

Variational Monte Carlo uses the stochastic integration method to evaluate the expectation value of the Hamiltonian for a chosen trial wave function, which depends on a set of variational parameters.

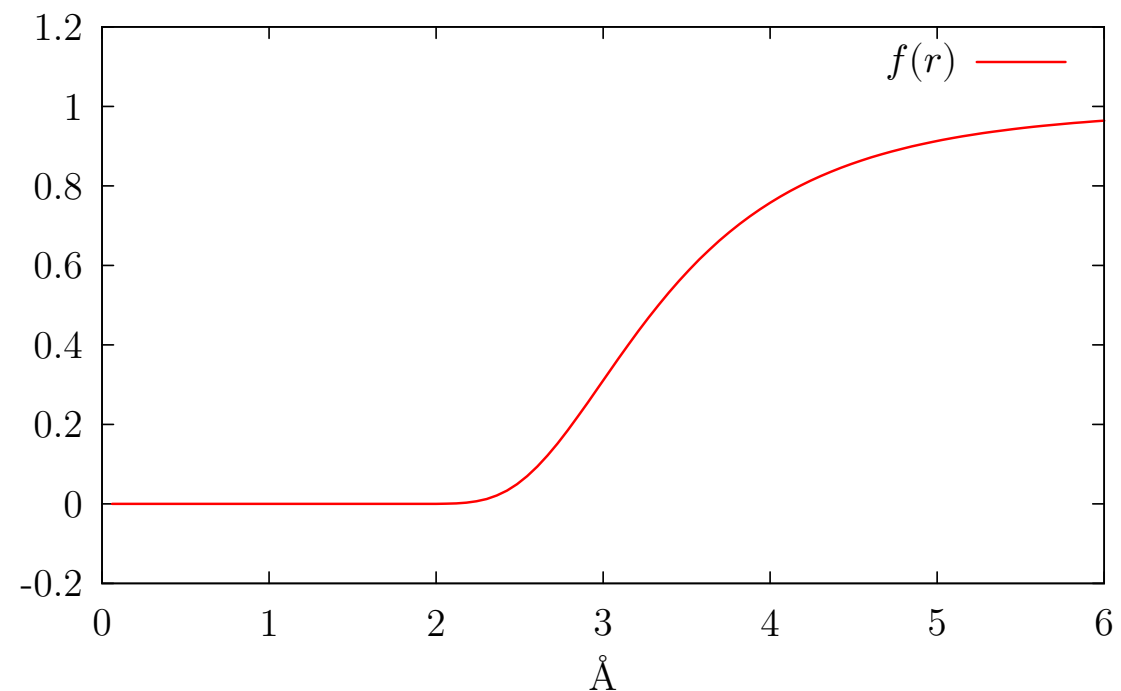
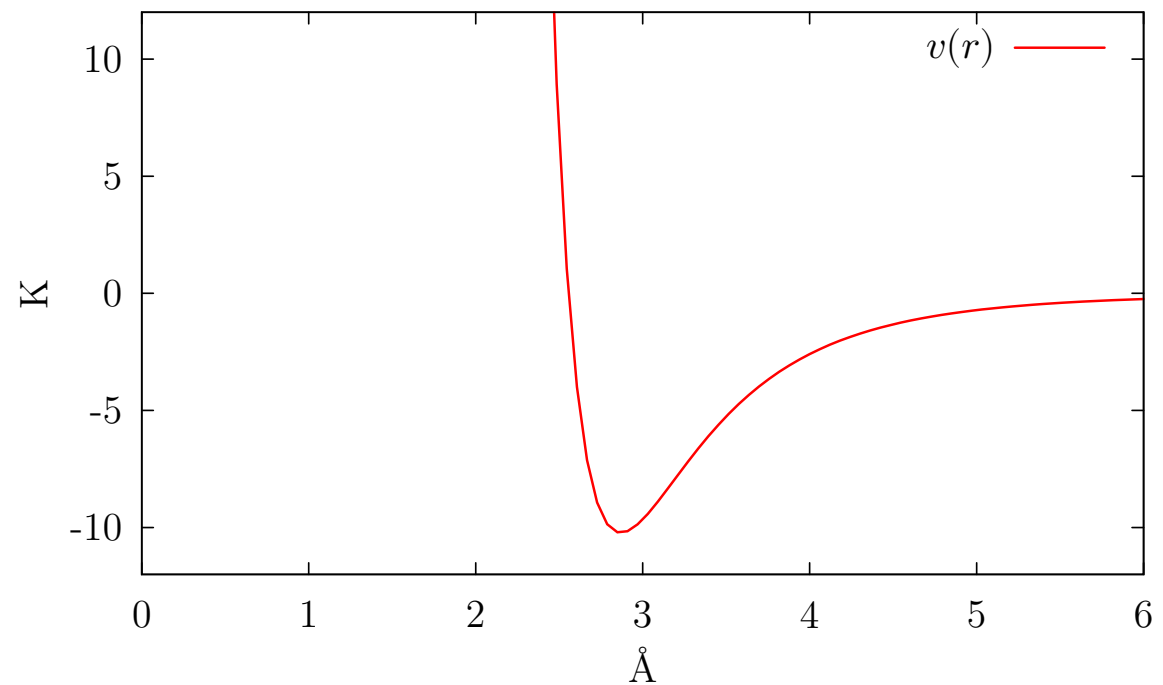
The interaction between ^4He atoms forming an homogeneous liquid can be parametrized by means of the two-body Lennard-Jones potential

$$v(r) = 4\epsilon \left[\left(\frac{\sigma}{r} \right)^{12} - \left(\frac{\sigma}{r} \right)^6 \right]$$

A reasonable trial wave function is small where the potential is repulsive and large where the potential is attractive

$$\Psi_T(R) = \prod_{i < j} f(r_{ij})$$

$$f(r) = \exp \left[-\frac{1}{2} \left(\frac{b}{r} \right)^5 \right]$$



Variational Monte Carlo

The variational principle guarantees that the energy of the trial wave function is greater than or equal to the ground-state energy with the same quantum numbers as

$$E_T = \frac{\langle \Psi_T | H | \Psi_T \rangle}{\langle \Psi_T | \Psi_T \rangle} \geq E_0$$

The variational parameters are determined by minimizing the trial energy. In the atomic liquid ^4He atoms case this amounts to

$$\frac{\partial E_T}{\partial b} = 0$$

Note that, in order to compute the trial energy for a given set of variational parameters, the following multi-dimensional integral in the degrees of freedom of the system (coordinates, spin and isospin) has to be evaluated

$$E_T = \frac{\int dR \Psi_T^*(R) H \Psi_T(R)}{\int dR \Psi_T^*(R) \Psi_T(R)}$$

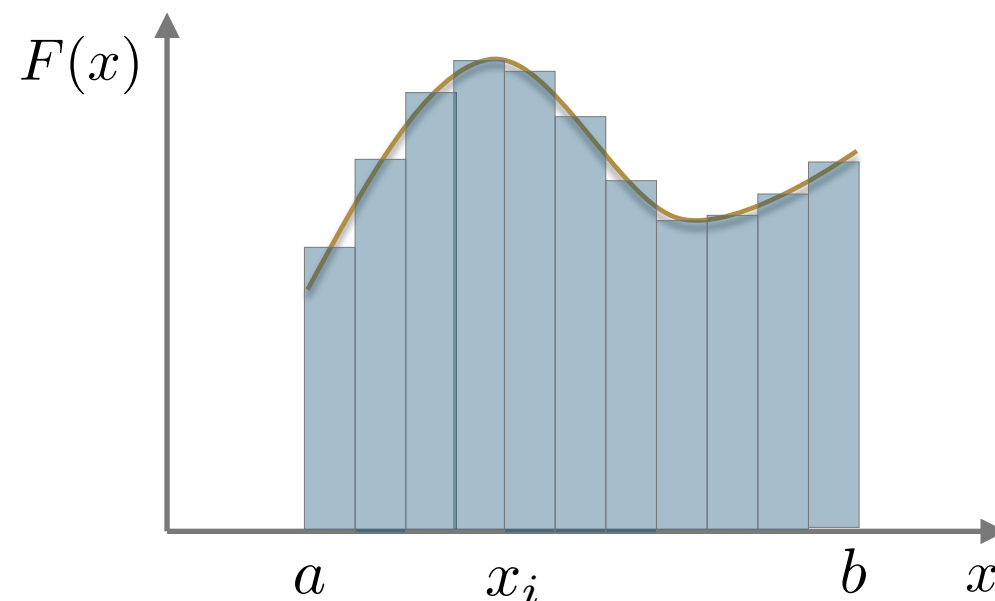
$$R \equiv \mathbf{r}_1, \dots, \mathbf{r}_A$$

Multi dimensional integrals

Our goal consists in computing the following D-dimensional integral

$$I(D) = \int_{a_1}^{b_1} dx_1 \dots \int_{a_D}^{b_D} dx_D F(x_1, \dots, x_D)$$

In the one-dimensional case, we can divide the area below to the curve into rectangles



$$\left\{ \begin{array}{l} I(1) \simeq h \sum_i F(x_i) \\ \Delta(1) = h^2 |F'(x_i)| + O(h^3) \\ h \propto \frac{1}{N} \end{array} \right.$$

How many points do we need to achieve a given precision ?

$$\frac{\Delta(1)}{I(1)} = \epsilon \quad \Rightarrow \quad N \propto \frac{1}{\epsilon}$$

Multi dimensional integrals

A generalization of the As for the D-dimensional case, it is easy to find

$$\left\{ \begin{array}{l} I(D) \simeq h^D \sum_i F(x_i) \\ \Delta(D) = h^{D+1} |\nabla F(x_i)| + O(h^{D+2}) \\ h \propto \frac{1}{N^D} \end{array} \right. \quad \Rightarrow \quad N \propto \frac{1}{\epsilon^D}$$

Note that more clever methods can be used, but the error is always proportional to h^α .

Problem

How many points do we need to compute the expectation value of the Hamiltonian for a system containing 12 particles interacting with a central potential with a precision $\epsilon = 0.1$?

Multi dimensional integrals

A generalization of the As for the D-dimensional case, it is easy to find

$$\left\{ \begin{array}{l} I(D) \simeq h^D \sum_i F(x_i) \\ \Delta(D) = h^{D+1} |\nabla F(x_i)| + O(h^{D+2}) \\ h \propto \frac{1}{N^D} \end{array} \right. \quad \Rightarrow \quad N \propto \frac{1}{\epsilon^D}$$

Note that more clever methods can be used, but the error is always proportional to h^α .

Problem

How many points do we need to compute the expectation value of the Hamiltonian for a system containing 12 particles interacting with a central potential with a precision $\epsilon = 0.1$?

Solution

Because the potential is central, we will be dealing with a 36-dimensional integral

$$D = 36 \quad \Rightarrow \quad N \propto 10^{36} \quad \Rightarrow \quad \boxed{10^{17} \text{ hours on Mira!!!}}$$

Monte Carlo quadrature

It clearly appears that standard numerical integration methods are not suitable to compute the energy per particle (and other relevant quantities) of ^{12}C !

Problem

What do we do?

Monte Carlo quadrature

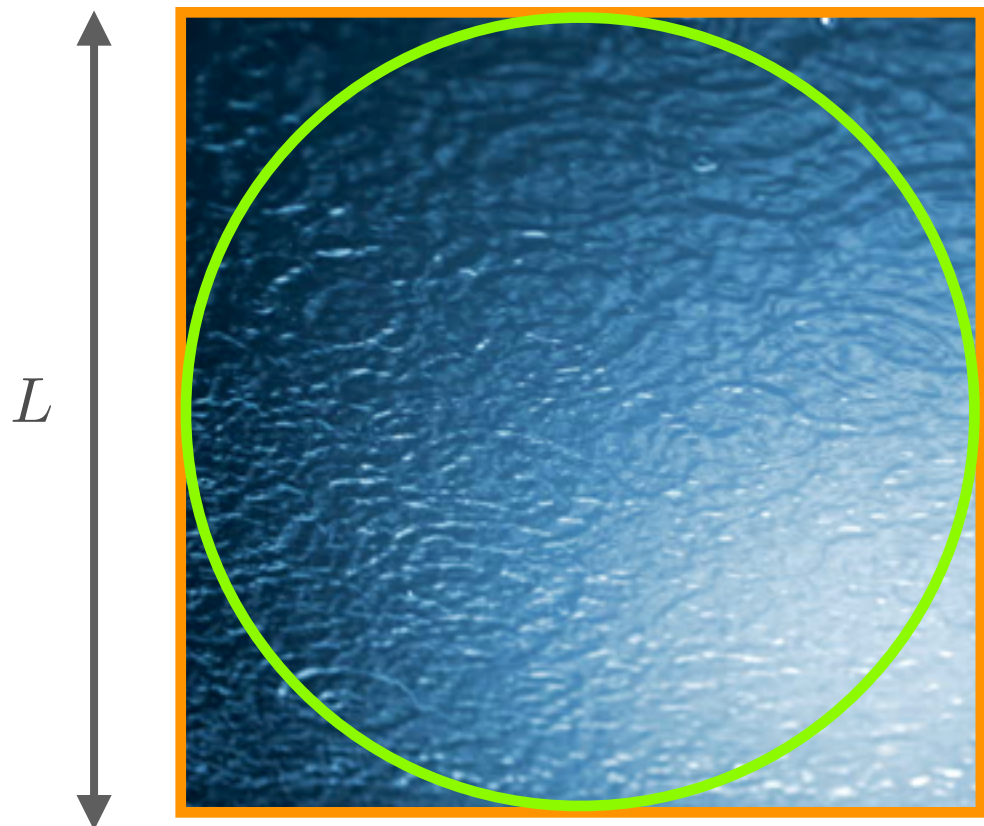
It clearly appears that standard numerical integration methods are not suitable to compute the energy per particle (and other relevant quantities) of ^{12}C !

Problem

What do we do?

Solution

We wait for the rain to fall, we collect raindrops and then we measure how much rain has fallen...



$$\frac{\text{Circle Area}}{\text{Square Area}} = \frac{\pi L^2 / 4}{L^2} = \frac{\pi}{4}$$

The central limit theorem

Suppose that the N continuum random variables x_1, \dots, x_N are drawn from the probability distribution $P(x)$ and consider the function $f(x)$. We may define a new random variable

$$S_N = \frac{1}{N} \sum_{i=1}^N f(x_i)$$

If the samples are statistically independent, the **central limit theorem** states that the probability distribution of S_N is gaussian

$$P(S_N) = \frac{1}{\sqrt{2\pi\sigma_N^2}} e^{-\frac{(S_N - \bar{S}_N)^2}{2\sigma_N^2}}$$

where the average and the variance of S_N are given by

$$\bar{S}_N = \int dx P(x) f(x) \quad \sigma_N = \sqrt{\frac{1}{N} \left[\int dx P(x) f^2(x) - \bar{S}_N^2 \right]}$$

These results hold true for any dimensionality of the space in which the variable x is defined !!!

The central limit theorem

Therefore, the central limit theorem provides a recipe to numerically evaluate multi-dimensional integrals of the form

$$I = \int dx f(x)$$

- Since the probability density has to be positive definite, rewrite the integral as:

$$I = \int dx P(x) \frac{f(x)}{P(x)}$$

- Sample N (with N “large”) points from the probability density $P(x)$
- Average the N values of $f(x_i)$ and $f^2(x_i)$

$$I = \frac{1}{N} \sum_{i=1}^N f(x_i) \pm \sqrt{\frac{1}{(N-1)} \left[\frac{1}{N} \sum_{i=1}^N f^2(x_i) - \left(\frac{1}{N} \sum_{i=1}^N f(x_i) \right)^2 \right]}$$

The central limit theorem

Two key aspects of Monte Carlo quadrature

- the error can be rigorously estimated
- the estimate of the error decreases as $1/\sqrt{N}$ regardless of the dimensionality

Problem

How many points do we need to sample to compute the expectation value of the Hamiltonian for a system containing 12 particles interacting with a central potential with a precision $\epsilon = 0.1$?

The central limit theorem

Two key aspects of Monte Carlo quadrature

- the error can be rigorously estimated
- the estimate of the error decreases as $1/\sqrt{N}$ regardless of the dimensionality

Problem

How many points do we need to sample to compute the expectation value of the Hamiltonian for a system containing 12 particles interacting with a central potential with a precision $\epsilon = 0.1$?

Solution

$$N \propto \epsilon^2 \simeq 100$$

Problem

And what about a system containing 36 particles (interacting with a central potential) ?

The central limit theorem

Two key aspects of Monte Carlo quadrature

- the error can be rigorously estimated
- the estimate of the error decreases as $1/\sqrt{N}$ regardless of the dimensionality

Problem

How many points do we need to sample to compute the expectation value of the Hamiltonian for a system containing 12 particles interacting with a central potential with a precision $\epsilon = 0.1$?

Solution

$$N \propto \epsilon^2 \simeq 100$$

Problem

And what about a system containing 36 particles (interacting with a central potential) ?

Solution

THE SAME !!!

Variational Monte Carlo

Remember that the numerator of the expectation value of the Hamiltonian for a system containing A particles interacting with a spin-independent potential reads

$$E_T = \int dR \Psi_T^*(R) H \Psi_T(R)$$

In order to use the central limit theorem, the former integral has to be rewritten as

$$E_T = \int dR |\Psi_T(R)|^2 E_L(R)$$

where we have defined the **local energy**

$$E_L(R) \equiv \frac{H \Psi_T(R)}{\Psi_T(R)}$$

Since it is positive and integrable, $|\Psi_T(R)|^2$ can be regarded as a probability density.

In order to compute the trial energy one has to find a way to sample $|\Psi_T(R)|^2$

M(RT)² algorithm

The algorithm was first described in a paper by Metropolis, Rosenbluth, Rosenbluth, Teller and Teller M(RT)². It shares common features to the rejection techniques because:

- It involves explicitly proposing a tentative value of the variable we want to sample, which may be rejected.
- The normalization of the sampled function is irrelevant.

M(RT)² algorithm has its own advantages and disadvantages:

Pros

- It can be used to sample essentially any density function regardless of analytic complexity in any number of dimensions
- It is of very great simplicity.

Cons

- Sampling is correct only asymptotically
- Consecutive variables produced are often very strongly correlated
- Not well suited to sample distributions with parameters that change frequently.

M(RT)² algorithm

To begin with, consider a 1-D harmonic oscillator. We want to sample the probability distribution described by the modulus squared of our trial wave function

$$P(x) \equiv |\Psi_T(x)|^2 \qquad \Psi_T(x) = \exp\left(-\alpha \frac{x^2}{2}\right)$$

M(RT)² algorithm is based on the idea of random walk in the space of the random variable x . The game consists of generating a random variable applying a transformation to another. This “moving” point is called walker.

$$P_{i+1}(x_{i+1}) = \int dx_i P_i(x_i) T(x_i \rightarrow x_{i+1})$$

Transition probability 

By recursively applying the same transformation we get

$$P_n(x_n) = \int dx_1 \dots dx_{n-1} P_1(x_1) T(x_1 \rightarrow x_2) \dots T(x_{n-1} \rightarrow x_n)$$

Under some very general conditions it can be proven that

$$\lim_{n \rightarrow \infty} P_n(x_n) = P(x) \Rightarrow \text{where } P(x) \text{ only depends on } T$$

M(RT)² algorithm

Let us impose a further condition, i.e. that the asymptotic distribution is an “equilibrium” state:

$$P(x)T(x \rightarrow y) = P(y)T(y \rightarrow x)$$

The latter is called detailed balance condition, because it does not hold only on average, but it tells that point by point there is no net flux of probability!

We can arbitrarily split the transition probability in two terms

$$T(x \rightarrow y) = G(x \rightarrow y)A(x \rightarrow y)$$

It describes the probability of moving the walker from $x \rightarrow y$.



It tells whether the proposed move is accepted or rejected.

The detailed balance then reads

$$\frac{A(y \rightarrow x)}{A(x \rightarrow y)} = \frac{P(x)G(x \rightarrow y)}{P(y)G(y \rightarrow x)}$$

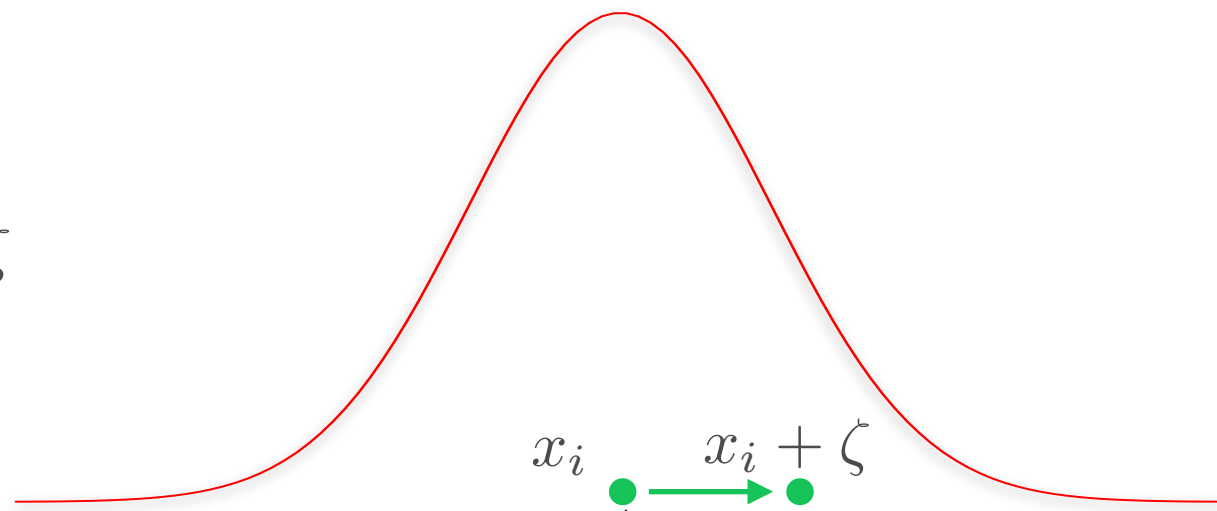
It can be easily checked that the following acceptance probability satisfies the above requirement

$$A(y \rightarrow x) = \min \left(1, \frac{P(x)G(x \rightarrow y)}{P(y)G(y \rightarrow x)} \right)$$

M(RT)² algorithm

In QMC we use a very simple prescription for $G(x \rightarrow y)$, which in 1-D corresponds to shifting a point by a value distributed according to a gaussian distribution

$$x_{i+1} = x_i + \zeta$$



In the many-particle case, the one dimensional gaussian is replaced by a three-dimensional one for each of the particles.

Since the probability of going from x to y is the same as the one for going from y to x , it turns out that

$$G(x \rightarrow y) = G(y \rightarrow x) \quad \longleftrightarrow \quad A(y \rightarrow x) = \min \left(1, \frac{P(x)}{P(y)} \right)$$

M(RT)² applied to VMC

At this point, we can describe the Metropolis algorithm for a VMC calculation in the 1-D case

Step 0 - Start from a “flat” distribution of walkers on the coordinate x

Step 1 - Move the walkers according to $G(x_i \rightarrow y_{i+1})$, i.e. $y_{i+1} = x_i + \zeta$

Step 2 - Compute the acceptance probability $A(x_i \rightarrow y_{i+1}) = \min \left(1, \frac{|\Psi_T(y_{i+1})|^2}{|\Psi_T(x_i)|^2} \right)$

Step 3 - Accept or reject the proposed move

$$\frac{|\Psi_T(y_{i+1})|^2}{|\Psi_T(x_i)|^2} > \xi \Rightarrow x_{i+1} = y_{i+1}$$

$$\frac{|\Psi_T(y_{i+1})|^2}{|\Psi_T(x_i)|^2} \leq \xi \Rightarrow x_{i+1} = x_i$$

But how do we sample from a Gaussian?

Fortran, C, Python, have their own random number generators. These generators provide you with random numbers ξ_i uniformly distributed between 0 and 1

Problem

Given ξ_1 and ξ_2 uniformly distributed between 0 and 1, how can we sample ζ from a normal gaussian distribution?

But how do we sample from a Gaussian?

Fortran, C, Python, have their own random number generators. These generators provide you with random numbers ξ_i uniformly distributed between 0 and 1

Problem

Given ξ_1 and ξ_2 uniformly distributed between 0 and 1, how can we sample ζ from a normal gaussian distribution?

Solution

We use the Box-Mueller method:

$$\zeta_1 = \sqrt{-2 \ln(1 - \xi_1)} \cos(2\pi\xi_2) \quad \zeta_2 = \sqrt{-2 \ln(1 - \xi_1)} \sin(2\pi\xi_2)$$

are both distributed according to

$$P(\zeta_i) = \frac{1}{\sqrt{2\pi}} e^{-\frac{\zeta_i^2}{2}}$$

The only drawback of this method is that it is fairly slow (but more than OK for our QMC purposes)

But how do we sample from a Gaussian?

```
function rgauss(irn)
implicit none
integer, parameter :: i8=selected_int_kind(15)
integer, parameter :: r8=selected_real_kind(15,9)
real(kind=r8) :: pi
real(kind=r8) :: rgauss,x1,x2
integer(kind=i8) :: irn
call ran(x1,irn)
call ran(x2,irn)
pi=4.0_r8*atan(1.0_r8)
rgauss=sqrt(-2.0_r8*log(x1))*cos(2.0_r8*pi*x2)
return
end
```

uniformly distributed between 0 and 1



And in practice the acceptance...

How do we sample the acceptance probability? Well, we first compute the ratio

$$\frac{|\Psi_T(y_{i+1})|^2}{|\Psi_T(x_i)|^2}$$

Then we roll the dice! We sample a random number ξ uniformly distributed between 0 and 1 and

$$\frac{|\Psi_T(y_{i+1})|^2}{|\Psi_T(x_i)|^2} > \xi \quad \text{Move accepted}$$

$$\frac{|\Psi_T(y_{i+1})|^2}{|\Psi_T(x_i)|^2} \leq \xi \quad \text{Move rejected}$$

$$\Psi_T(x) = \exp(-\alpha x^2/2)$$

```
Accepted → prob=exp(-alpha*(xnew**2-xo(n)**2))
             call ran(csi,irn)
             if (csi.lt.prob) then
                 eloc=-0.5_r8*((alpha*xnew)**2-alpha)+0.5_r8*omega**2*xnew**2
                 xn(n)=xnew
                 nacc=nacc+1
Rejected → else
             eloc=-0.5_r8*((alpha*xo(n))**2-alpha)+0.5_r8*omega**2*xo(n)**2
             xn(n)=xo(n)
             endif
```

M(RT)² applied to VMC

Problem (at this point duable!)

Given the 1-D harmonic oscillator Hamiltonian

$$H = -\frac{1}{2} \frac{d^2}{dx^2} + \frac{x^2}{2}$$

find the optimal variational parameter of the following trial wavefunction

$$\Psi_T(X) = \exp\left(-\alpha \frac{x^2}{2}\right)$$

M(RT)² applied to VMC

Problem (at this point duable!)

Given the 1-D harmonic oscillator Hamiltonian

$$H = -\frac{1}{2} \frac{d^2}{dx^2} + \frac{x^2}{2}$$

find the optimal variational parameter of the following trial wavefunction

$$\Psi_T(X) = \exp\left(-\alpha \frac{x^2}{2}\right)$$

Solution

- Use the M(RT)² described earlier to sample the position x_i of the walkers
- After some “equilibration” steps, compute the local energy of a given configuration

$$E_L(x_i) = \frac{H\Psi_T(x_i)}{\Psi_T(x_i)} = \frac{\alpha}{2} + \frac{x_i^2}{2} [1 - \alpha^2]$$

- Accumulate statistics, try a new σ and iterate!

Nuclear VMC wave function

A good trial wave function to describe a nucleus has to reflect the complexity of the nuclear potential

It contains 3-body correlations stemming from 3-body potential

$$\Psi_T = \left[1 + \sum_{i < j < k} \tilde{U}_{ijk}^{\text{TNI}} \right] \Psi_P \longleftrightarrow \tilde{U}_{ijk} \equiv \tilde{\epsilon}_A V_{ijk}^A + \tilde{\epsilon}_R V_{ijk}^R$$

The pair correlated wave function is written in terms of operator correlations arising from the 2-body potential

$$\Psi_P = \left[\mathcal{S} \prod_{i < j} (1 + U_{ij}) \right] \Psi_J \longleftrightarrow U_{ij} = \sum_{p=2,6} u^p(r_{ij}) O_{ij}^p$$

The total antisymmetric Jastrow wave function depends on the quantum numbers of the given nucleus

$$\Psi_J = \left[\prod_{i < j < k} f_{ijk}^c \right] \left[\prod_{i < j} f_{ij}^c \right] \Phi_A(J, M, T, T_3)$$

Green's Function Monte Carlo

- A walker associated with wave function of the nucleus, do not only describes the positions of the protons and neutrons, but also their spin and isospin!
- The GFMC wave function is written as a complex vector, the coordinates of which represent a spin-isospin state of the system
- The ${}^3\text{H}$ case fits in the slide!

$$|\Psi_{3H}\rangle = \begin{pmatrix} a_{\uparrow\uparrow\uparrow} \\ a_{\uparrow\uparrow\downarrow} \\ a_{\uparrow\downarrow\uparrow} \\ a_{\uparrow\downarrow\downarrow} \\ a_{\downarrow\uparrow\uparrow} \\ a_{\downarrow\uparrow\downarrow} \\ a_{\downarrow\downarrow\uparrow} \\ a_{\downarrow\downarrow\downarrow} \end{pmatrix} \otimes \begin{pmatrix} a_{pnn} \\ a_{npn} \\ a_{nnp} \end{pmatrix}$$

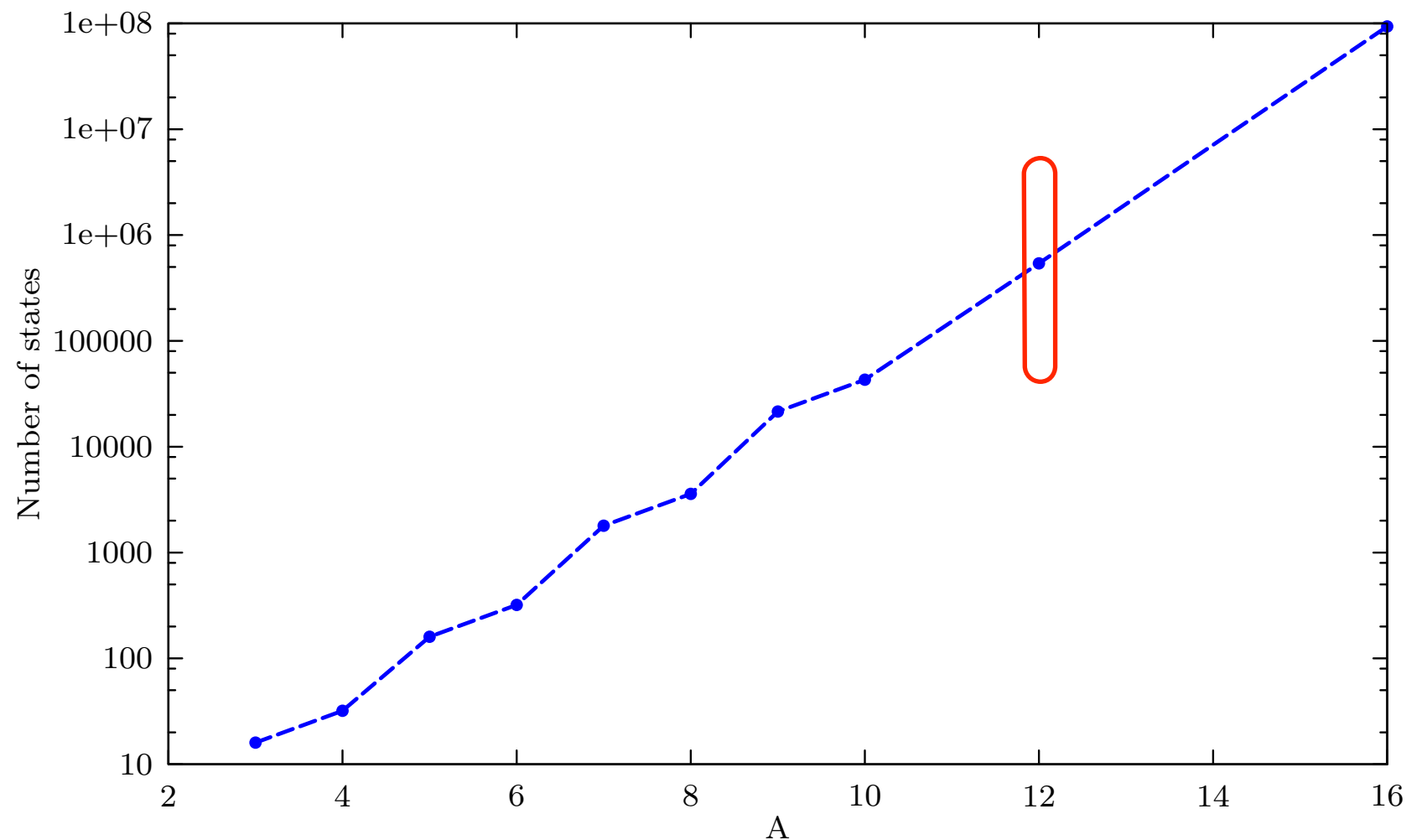
Green's Function Monte Carlo

The wave function can be expressed as a sum over spin-isospin states

$$|\Psi_0(\mathbf{r}_1 \dots \mathbf{r}_A)\rangle = \sum_{\alpha=1}^N \Psi_0^\alpha(\mathbf{r}_1 \dots \mathbf{r}_A) |\alpha\rangle$$

Question (easy)

How does the number of spin-states grow with the number of particles?



Green's Function Monte Carlo

The wave function can be expressed as a sum over spin-isospin states

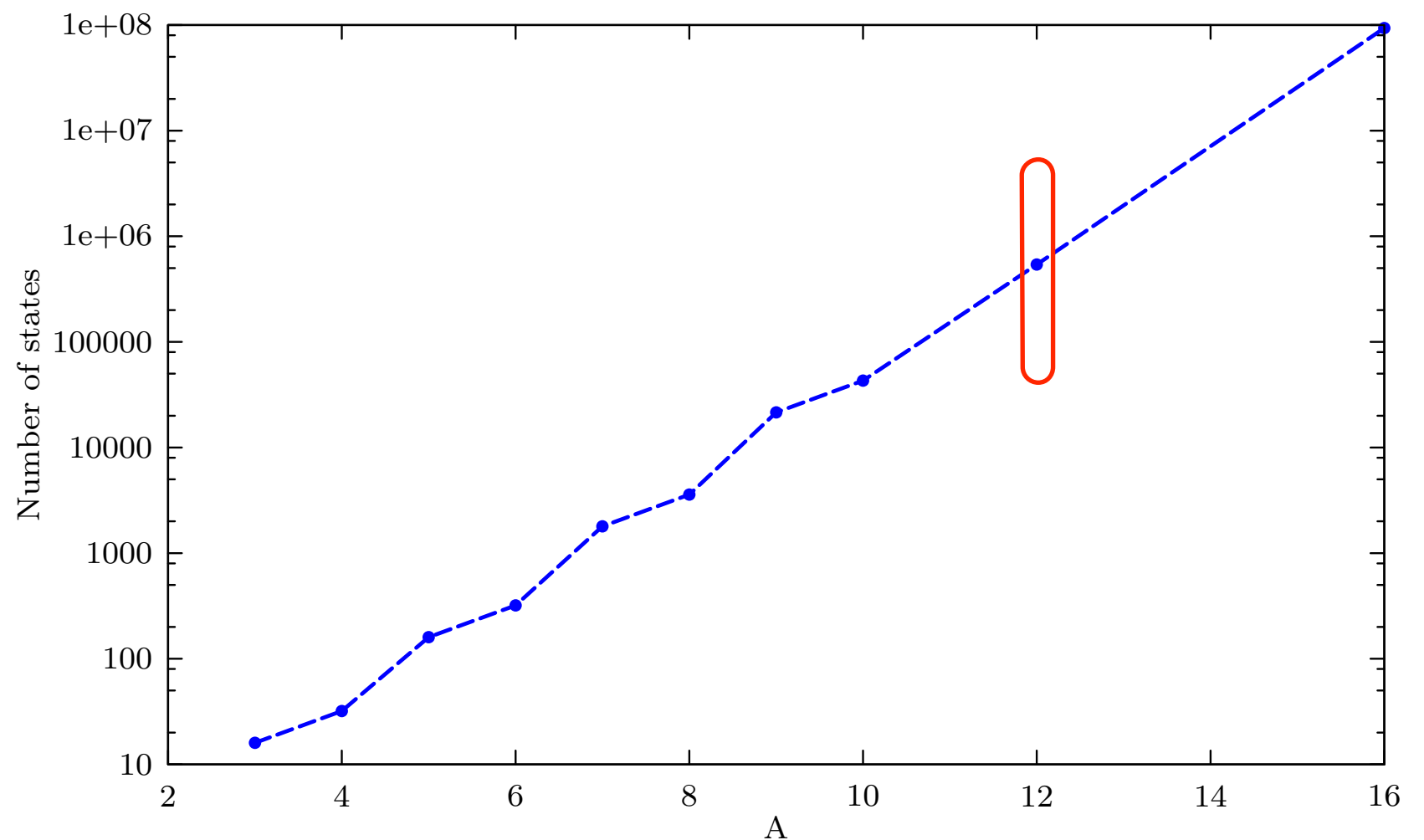
$$|\Psi_0(\mathbf{r}_1 \dots \mathbf{r}_A)\rangle = \sum_{\alpha=1}^N \Psi_0^\alpha(\mathbf{r}_1 \dots \mathbf{r}_A) |\alpha\rangle$$

Question (easy)

How does the number of spin-states grow with the number of particles?

Solution

$$2^A$$



Green's Function Monte Carlo

The wave function can be expressed as a sum over spin-isospin states

$$|\Psi_0(\mathbf{r}_1 \dots \mathbf{r}_A)\rangle = \sum_{\alpha=1}^N \Psi_0^\alpha(\mathbf{r}_1 \dots \mathbf{r}_A) |\alpha\rangle$$

Question (easy)

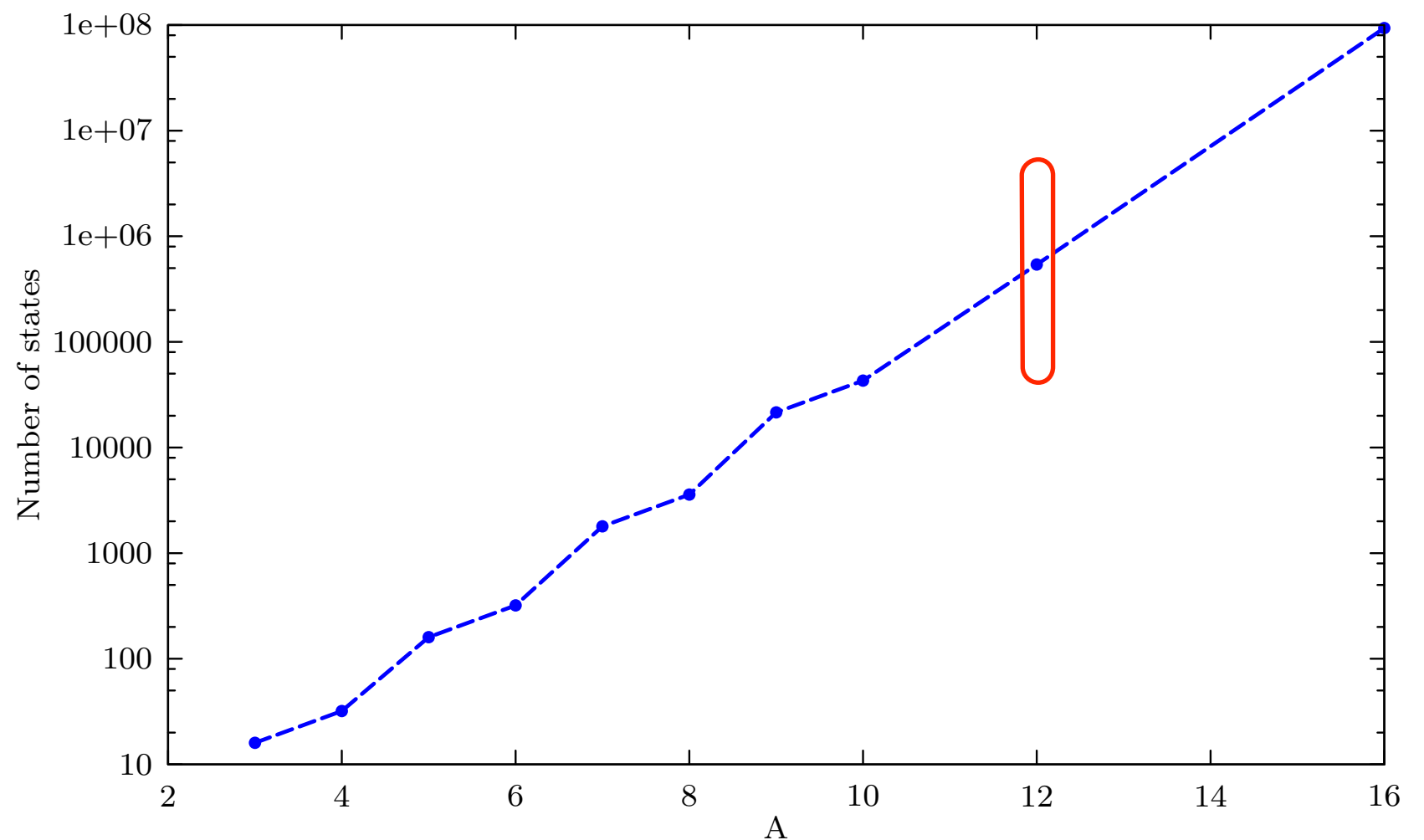
How does the number of spin-states grow with the number of particles?

Solution

$$2^A$$

Question (not so easy)

What about the number of states in the charge basis?



Green's Function Monte Carlo

The wave function can be expressed as a sum over spin-isospin states

$$|\Psi_0(\mathbf{r}_1 \dots \mathbf{r}_A)\rangle = \sum_{\alpha=1}^N \Psi_0^\alpha(\mathbf{r}_1 \dots \mathbf{r}_A) |\alpha\rangle$$

Question (easy)

How does the number of spin- states grow with the number of particles?

Solution

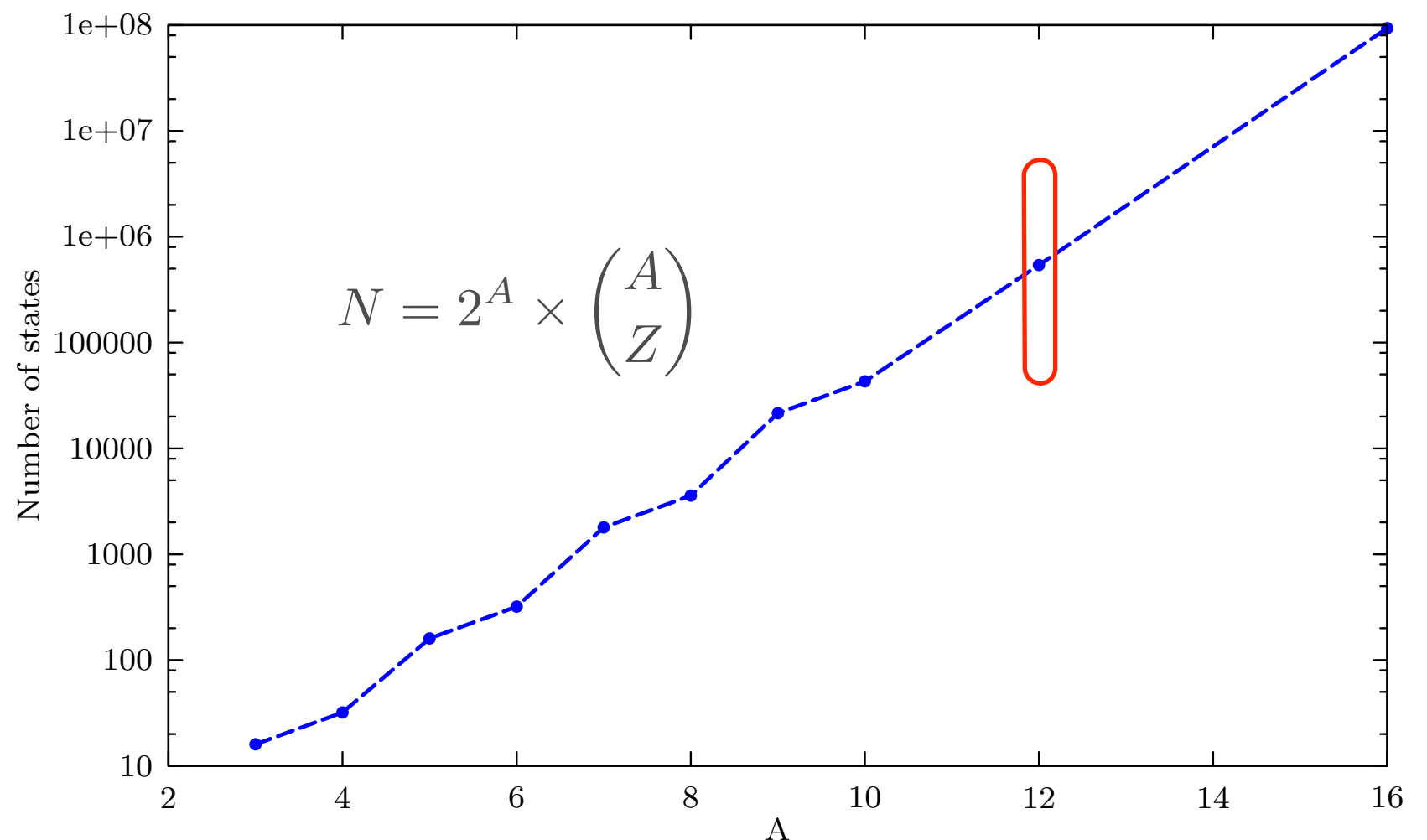
$$2^A$$

Question (not so easy)

What about the number of states in the charge basis?

Solution

$$\binom{A}{Z}$$



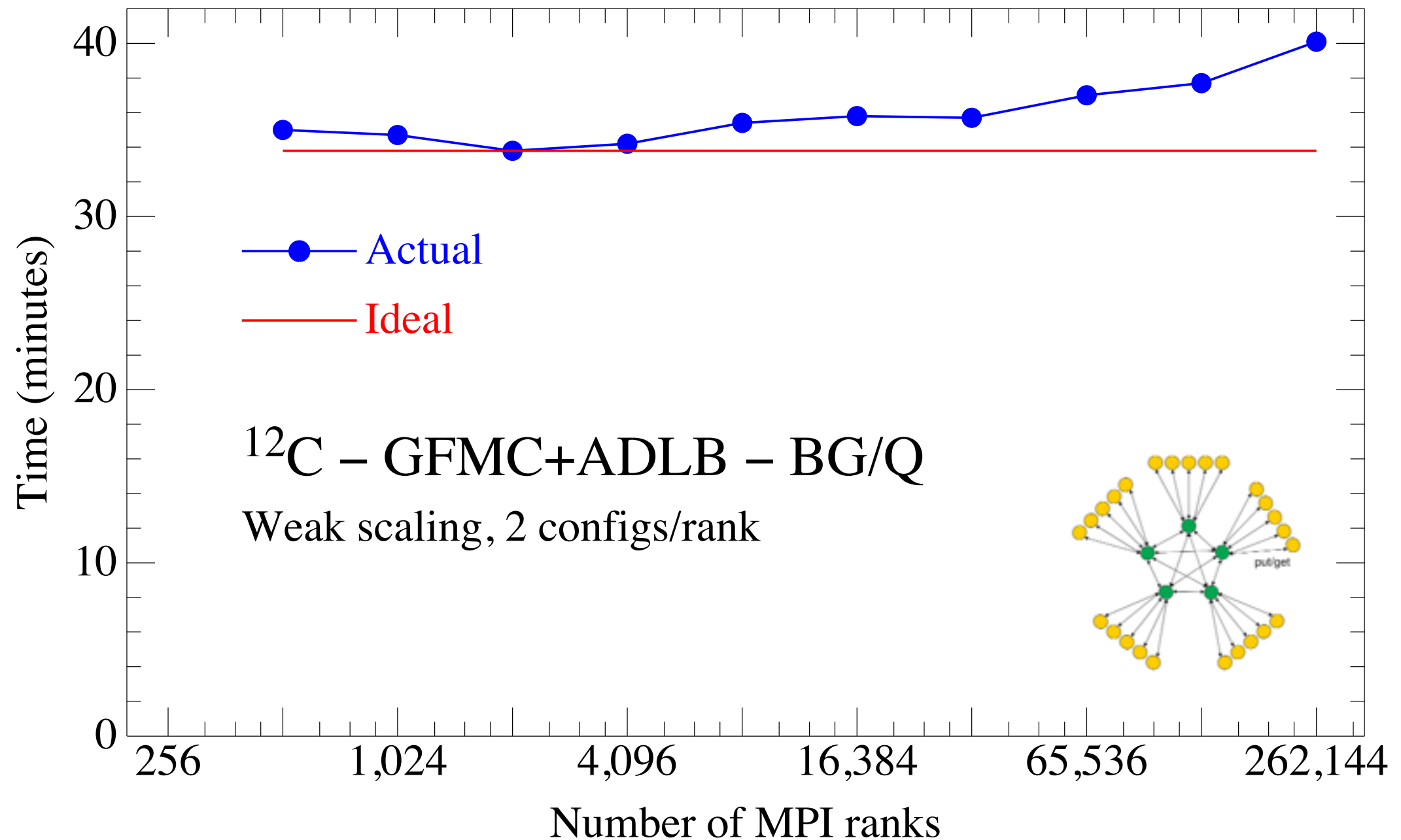
Need to go beyond MPI

- GFMC has steadily undergone development to take advantage of each new generation of parallel machine and was one of the first to deliver new scientific results each time.



Using supercomputers

- GFMC has steadily undergone development to take advantage of each new generation of parallel machine and was one of the first to deliver new scientific results each time.



Chapter 4

Diffusion Monte Carlo

Diffusion Monte Carlo

- The accuracy of a VMC calculation is limited by the knowledge of the trial wave function.
- The **diffusion Monte Carlo (DMC)** method, overcomes this limitation by using a projection technique to enhance the true ground-state component of a starting trial wave function.
- The method relies on the observation that the trial wave function can be expanded in the complete set of eigenstates of the the hamiltonian according to

$$|\Psi_T\rangle = \sum_n c_n |\Psi_n\rangle \qquad H|\Psi_n\rangle = E_n |\Psi_n\rangle$$

which implies

$$\lim_{\tau \rightarrow \infty} e^{-(H-E_0)\tau} |\Psi_T\rangle = c_0 |\Psi_0\rangle$$

where τ is the imaginary time. Hence, DMC projects out the exact lowest-energy state, provided the trial wave function it is not orthogonal to the ground state.

Diffusion Monte Carlo

- The direct calculation of $e^{-(H-E_0)\tau}$ for strongly-interacting systems involves prohibitive difficulties
- To circumvent this problem, the imaginary-time evolution is broken into N small imaginary-time steps, and complete sets of states are inserted

$$e^{-(H-E_0)\tau} |\Psi_T\rangle = \int dR_1 \dots dR_N |R_N\rangle \langle R_N| e^{-(H-E_0)\Delta\tau} |R_{N-1}\rangle \dots \\ \dots \langle R_2| e^{-(H-E_0)\Delta\tau} |R_1\rangle \Psi_T(R_1)$$

Note the analogy with the Feynman's path integrals in quantum and statistical mechanics !!!

- At imaginary-time $\tau_{i+1} = (i+1)\Delta\tau$ the walkers are distributed according to

$$\Psi(\tau_{i+1}, R_{i+1}) = \int dR_i \langle R_{i+1}| e^{(H-E_0)\Delta\tau} |R_i\rangle \Psi(\tau_i, R_i)$$

Diffusion Monte Carlo

The problem is then reduced to computing the **short-time Green's function** of the system

$$G(R_i \rightarrow R_{i+1}, \Delta\tau) = \langle R_i | e^{-(H-E_0)\Delta\tau} | R_{i+1} \rangle$$

The analytic solution of Green's function of the full hamiltonian is in general not known. An approximation to the Green's function can be obtained using the **Trotter Suzuki formula**

$$\langle R_i | e^{-(T+V-E_0)\Delta\tau} | R_{i+1} \rangle = e^{E_0\Delta\tau} \langle R_i | e^{-T\Delta\tau} e^{-V\Delta\tau} | R_{i+1} \rangle + \mathcal{O}(\Delta\tau^2)$$

In the limit of small time-step, the Green's function factorizes

$$G(R_i \rightarrow R_{i+1}, \Delta\tau) \simeq G_d(R_i \rightarrow R_{i+1}, \Delta\tau) G_b(R_i \rightarrow R_{i+1}, \Delta\tau)$$

Diffusion Monte Carlo

The **free Green's function** satisfies the master equation of a diffusion stochastic process

$$-\frac{\partial}{\partial \tau} G_d(R_i \rightarrow R_{i+1}, \Delta \tau) = -\frac{\hbar^2}{2m} \nabla^2 G_d(R_i \rightarrow R_{i+1}, \Delta \tau)$$

It is given by a 3A-dimensional Gaussian describing the Brownian diffusion of A particles with a dynamic governed by random collisions

$$G_d(R_i \rightarrow R_{i+1}, \Delta \tau) = \left(\frac{m}{2\pi \hbar^2 \Delta \tau} \right)^{\frac{3A}{2}} e^{-\frac{m}{2\hbar^2 \Delta \tau} (R_i - R_{i+1})^2}$$

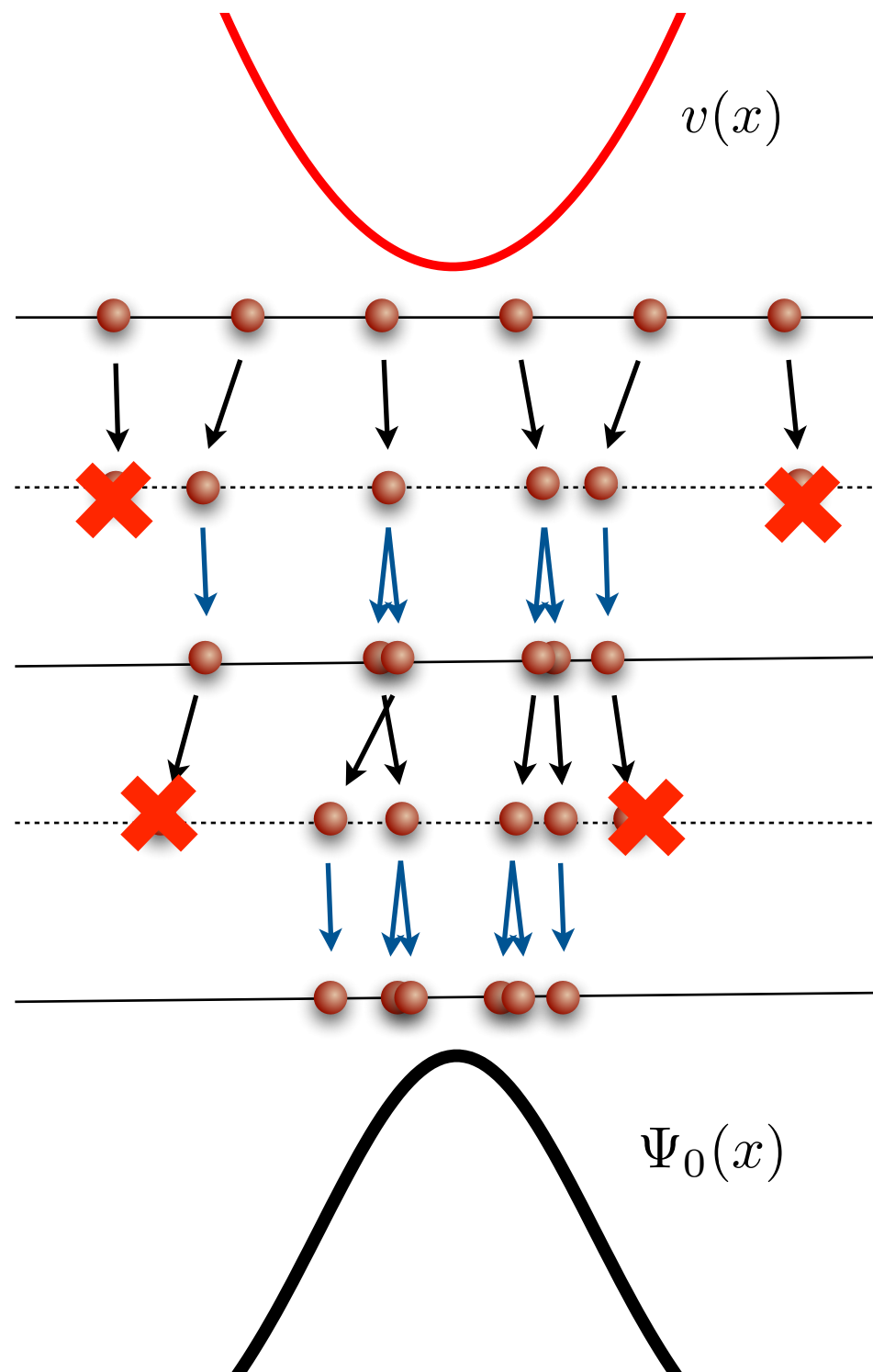
The **branching Green's function**, on the other hand, is simply given by

$$G_b(R_i \rightarrow R_{i+1}, \Delta \tau) = e^{-[V(R_{i+1}) - E_0] \Delta \tau}$$

Hence, at the imaginary time $\tau_{i+1} = (i + 1) \Delta \tau$ the walkers are distributed according to

$$\Psi(\tau_{i+1}, R_{i+1}) = \left(\frac{m}{2\pi \hbar^2 \Delta \tau} \right)^{\frac{3A}{2}} \int dR_i e^{-\frac{m}{2\hbar^2 \Delta \tau} (R_i - R_{i+1})^2} e^{-[V(R_{i+1}) - E_0] \Delta \tau} \Psi(\tau_i, R_i)$$

Diffusion Monte Carlo



- A set of walkers is sampled from the trial wave function

- Gaussian drift for the kinetic energy

$$\left(\frac{m}{2\pi\hbar^2\Delta\tau} \right)^{\frac{1}{2}} e^{-\frac{m}{2\hbar^2\Delta\tau}(x_i - x_{i+1})^2}$$

- Branching and killing of the walkers induced by the potential weight

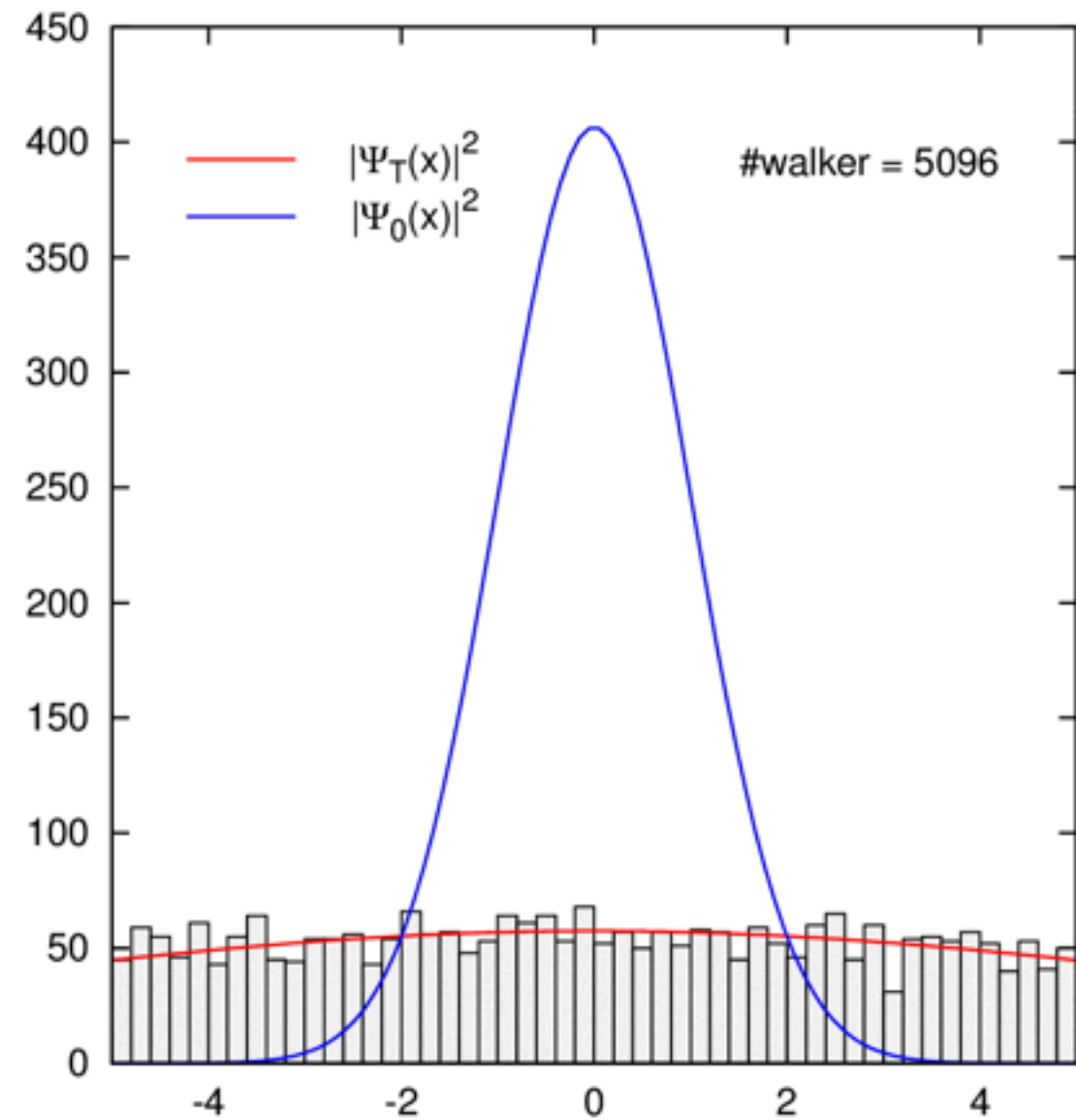
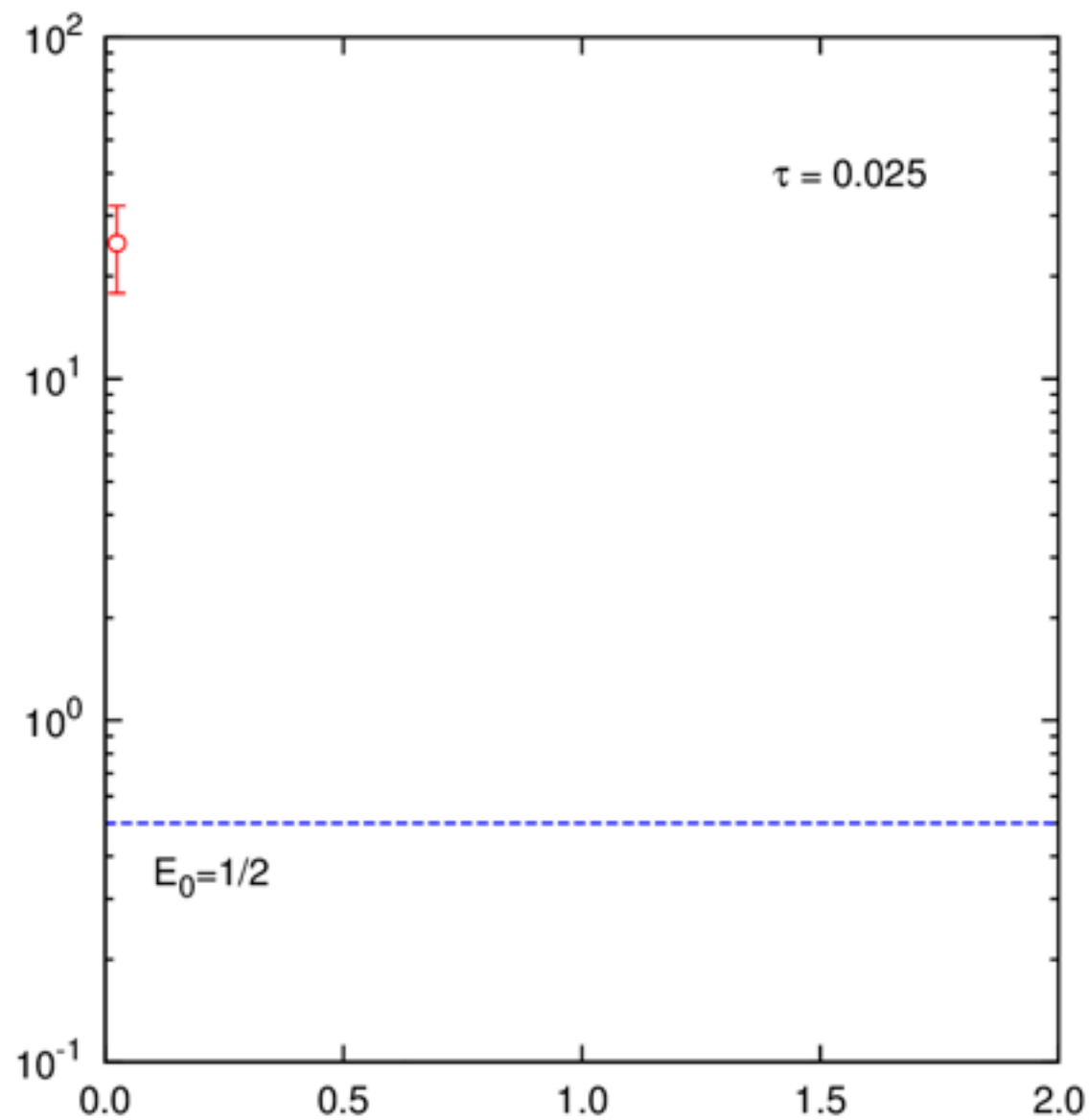
$$w(x_{i+1}) = e^{-[V(x_{i+1}) - E_0]\Delta\tau}$$

- Ground-state expectation values are estimated during the diffusion

$$\langle H \rangle = \frac{\sum_{x_i} \langle x_i | H | \Psi_T \rangle w(x_i)}{\sum_{x_i} \langle x_i | \Psi_T \rangle w(x_i)}$$

DMC for the 1d harmonic oscillator

$$H = -\frac{1}{2} \frac{d^2}{dx^2} + \frac{x^2}{2} \longleftrightarrow \begin{aligned} \Psi_0(x) &= e^{-x^2/2} \\ E_0 &= 1/2 \end{aligned}$$



Importance sampling

The algorithm as it was shown so far is not suitable for potentials presenting a divergent behavior

- A strongly repulsive potential (e.g. repulsive Coulomb, Lennard-Jones, Argonne v_{18}) will result in a very fast absorption of walkers, eventually killing the whole population.
- An attractive potential (e.g. Coulomb attraction between the nucleus and electrons in an atom) will generate an exponentially growing population

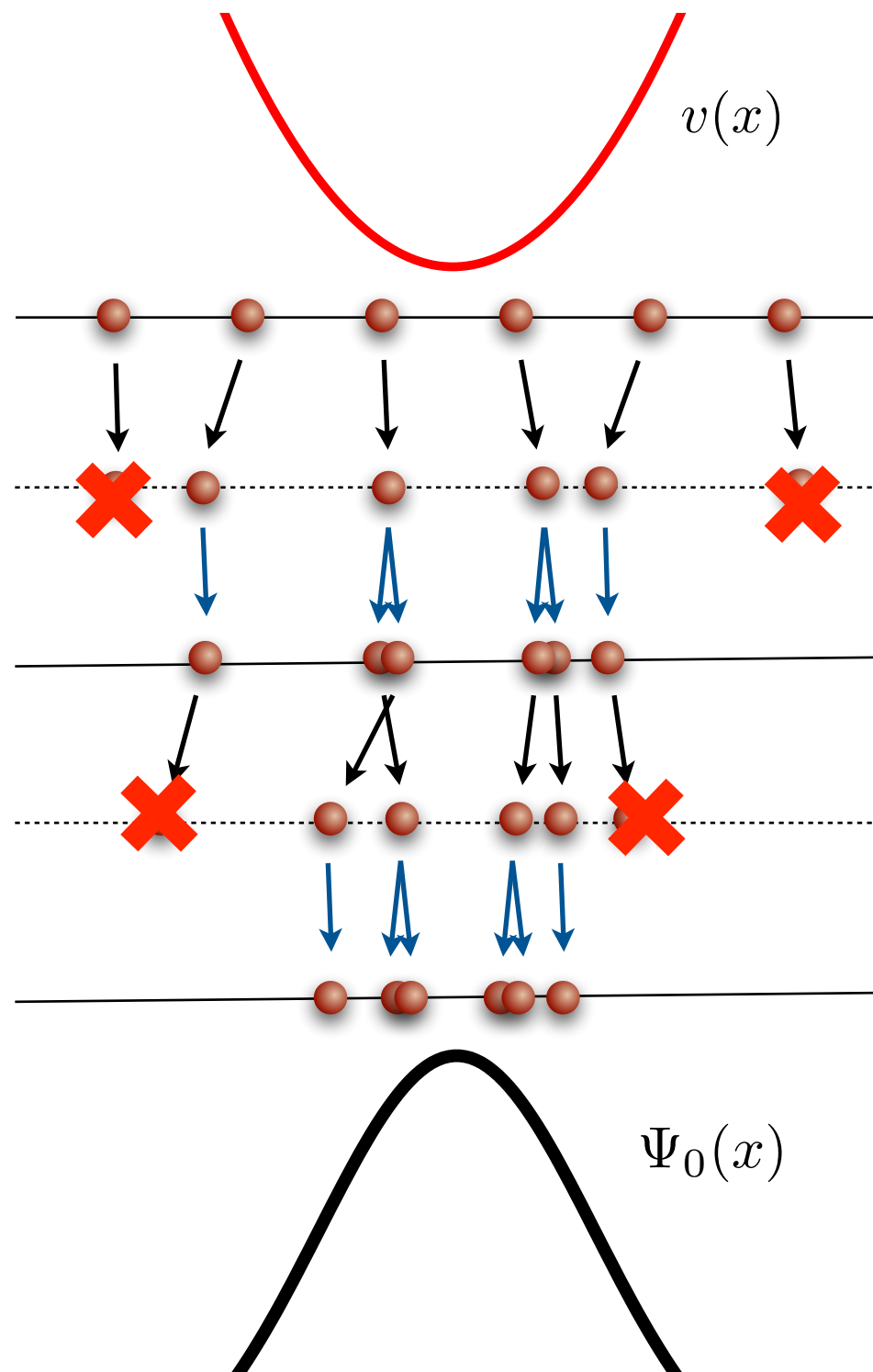
The idea of the importance sampling technique consists in using the knowledge of the trial wave function to guide the imaginary-time projection. Consider

$$f(\tau_i, R_i) \equiv \Psi_T(R_i)\Psi(\tau_i, R_i)$$

Its imaginary-time evolution is given by

$$f(\tau_{i+1}, R_{i+1}) = \int dR_i G_d(R_i \rightarrow R_{i+1}, \Delta\tau) G_b(R_i \rightarrow R_{i+1}, \Delta\tau) \frac{\Psi_T(R_{i+1})}{\Psi_T(R_i)} f(\tau_i, R_i)$$

Importance sampling diffusion Monte Carlo



- A set of walkers is sampled from the trial wave function

- Gaussian drift for the kinetic energy

$$\left(\frac{m}{2\pi\hbar^2\Delta\tau} \right)^{\frac{1}{2}} e^{-\frac{m}{2\hbar^2\Delta\tau}(x_i - x_{i+1})^2}$$

- Branching and killing of the walkers induced by the potential weight

$$w(x_i) = e^{-[V(x_{i+1}) - E_0]\Delta\tau} \frac{\Psi_T(x_{i+1})}{\Psi_T(x_i)}$$

- Ground-state expectation values are estimated during the diffusion

$$\langle H \rangle = \frac{\sum_{x_i} \frac{\langle x_i | H | \Psi_T \rangle}{\langle x_i | \Psi_T \rangle} w(x_i)}{\sum_{x_i} w(x_i)}$$

Importance sampling diffusion Monte Carlo

The importance sampling can also be implemented by adding a drift in the free Green's function

$$\tilde{G}_d(R_i \rightarrow R_{i+1}, \Delta\tau) = \left(\frac{m}{2\pi\hbar^2\Delta\tau} \right)^{\frac{3A}{2}} e^{-\frac{m}{2\hbar^2\Delta\tau} [R_i - R_{i+1} - \frac{\hbar^2\Delta\tau}{m} v_D(R_{i+1})]^2}$$

where the drift velocity is given by

$$v_D(R) = \frac{\nabla\Psi_T(R)}{\Psi_T(R)}$$

The branching Green's function is also modified according to

$$\tilde{G}_b(R_i \rightarrow R_{i+1}, \Delta\tau) = e^{-[E_L(R_{i+1}) - E_0]\Delta\tau} \longleftrightarrow E_L(R) = \frac{H\Psi_T(R)}{\Psi_T(R)}$$

Question

What is the most efficient implementation?

Solution

It depends on the problem. In general, the latter is the most efficient, as the diffusion process is driven by the trial wave function. Also, the local energy is more stable than the potential energy.

There is a LOT more to say...

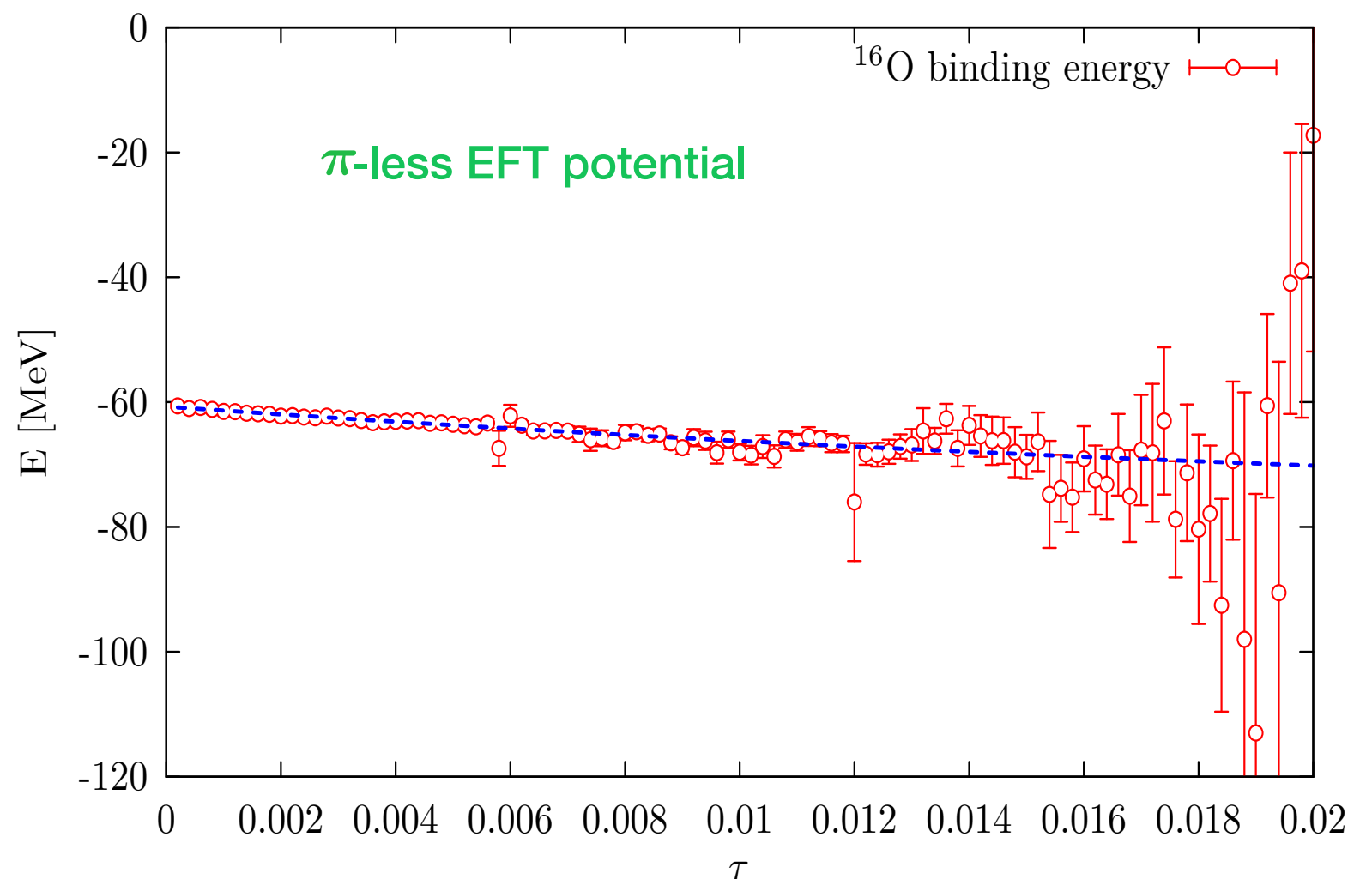
So far we have implicitly assumed that the wave function can be given a probabilistic interpretation, **but** a fermionic wave function is NOT positive definite. In the nuclear case it is not even real!

Since the ground-state of a given Hamiltonian is always bosonic, searching for the ground-state energy of a fermionic system is very similar to project onto an excited state.

However, since we are projecting onto an antisymmetric trial wave function, what really happens is that energy converges to exact eigenvalue with an exponentially growing statistical error. In other words, the signal to noise ratio decays exponentially.

This issue, known as **sign problem**, is common to all Monte Carlo approaches when applied to fermionic system, including Lattice

Many workarounds: fixed node, constrained path... but no definitive solution so far.



Chapter 5

How do we compute the electroweak response functions?

Integral transform techniques

- We want to compute the following response functions (nonrelativistic limit of the hadronic tensor)

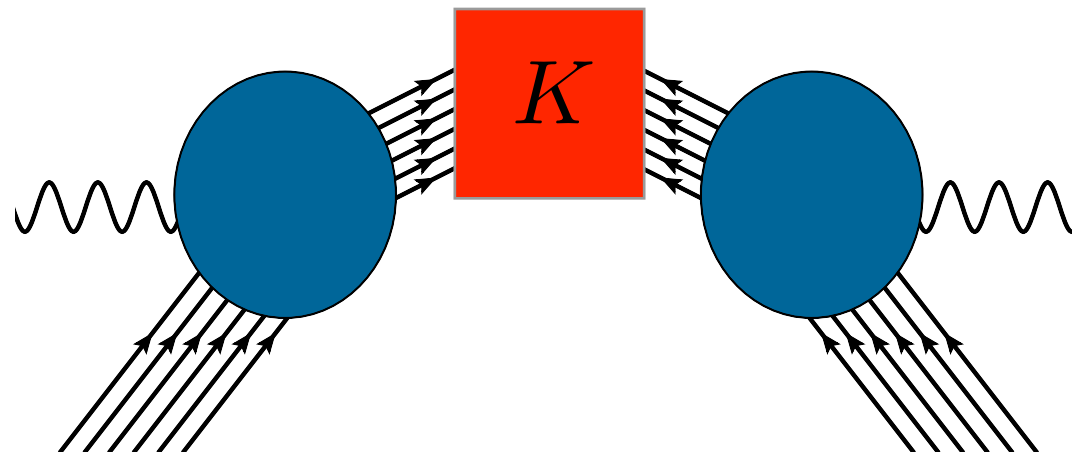
$$R_{\alpha\beta}(\omega, \mathbf{q}) = \sum_f \langle \Psi_0 | J_\alpha^\dagger(\mathbf{q}) | \Psi_f \rangle \langle \Psi_f | J_\beta(\mathbf{q}) | \Psi_0 \rangle$$

- The integral transform of the response function are generally defined as

$$E_{\alpha\beta}(\sigma, \mathbf{q}) \equiv \int d\omega K(\sigma, \omega) R_{\alpha\beta}(\omega, \mathbf{q})$$

- Using the completeness of the final states, they can be expressed in terms of ground-state expectation values

$$E_{\alpha\beta}(\sigma, \mathbf{q}) = \langle \Psi_0 | J_\alpha^\dagger(\mathbf{q}) K(\sigma, H - E_0) J_\beta(\mathbf{q}) | \Psi_0 \rangle$$



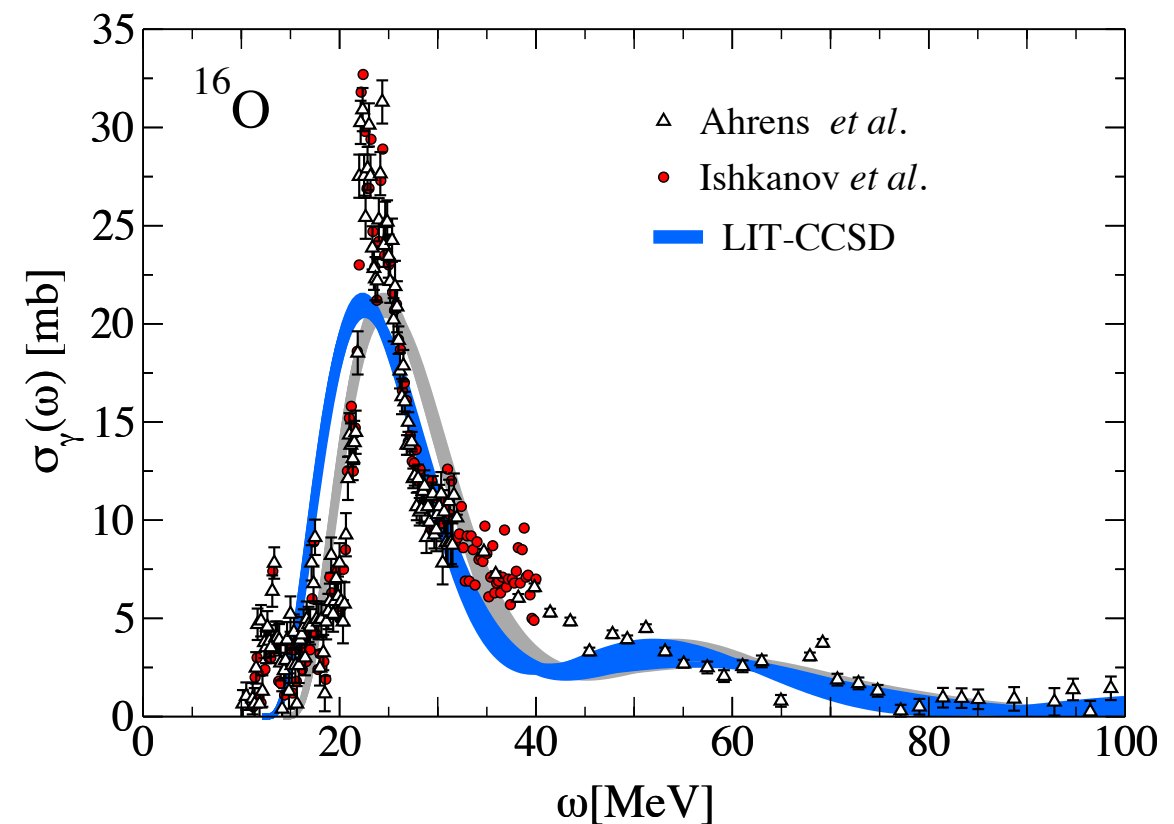
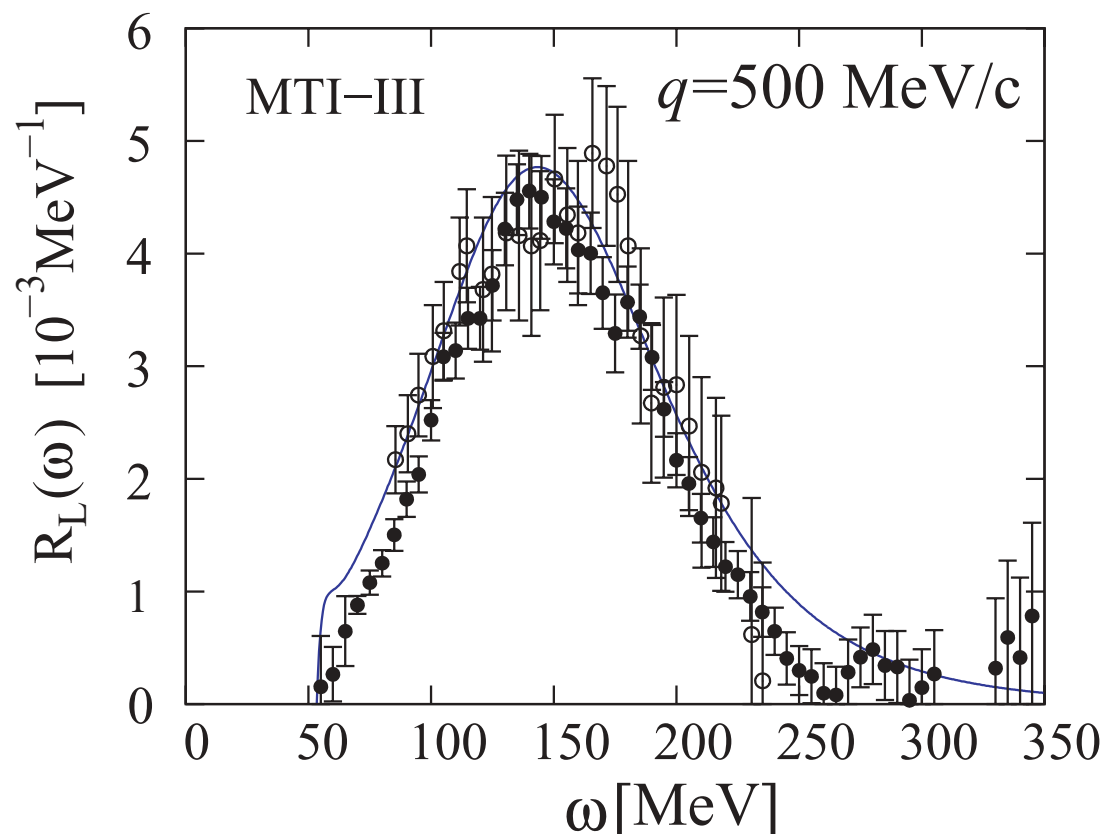
Lorentz integral transform (LIT)

- The Lorentz integral transform

$$K(\sigma, \omega) = \frac{1}{(\omega - \sigma_R)^2 + \sigma_I^2}$$

has been successfully exploited in the calculation of electromagnetic and neutral-weak responses of light nuclei.

- More recently, in combination with the coupled-cluster method, Lorentz integral transform has been applied to compute the giant dipole resonances of nuclei as large as ^{16}O , ^{22}O and ^{40}Ca .

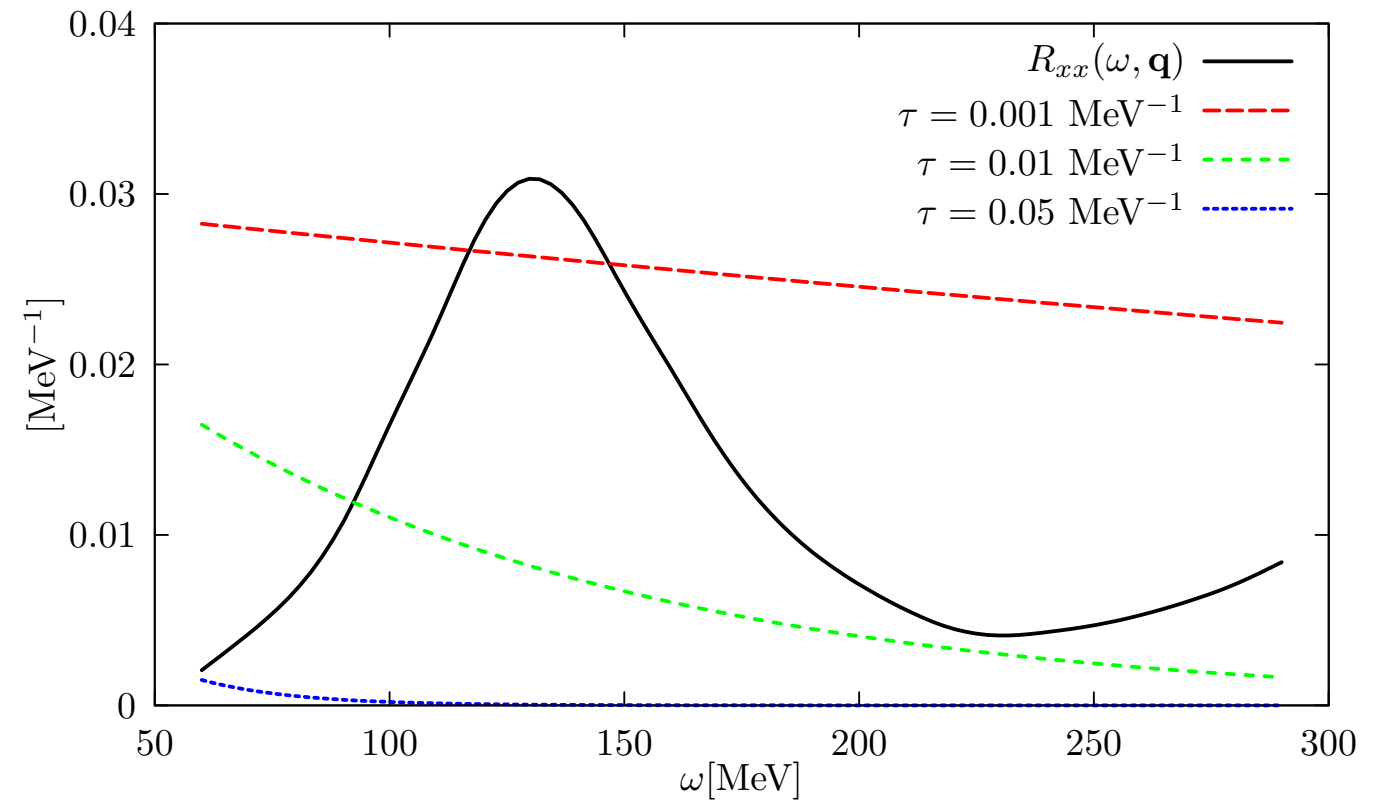


Euclidean response function

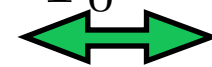
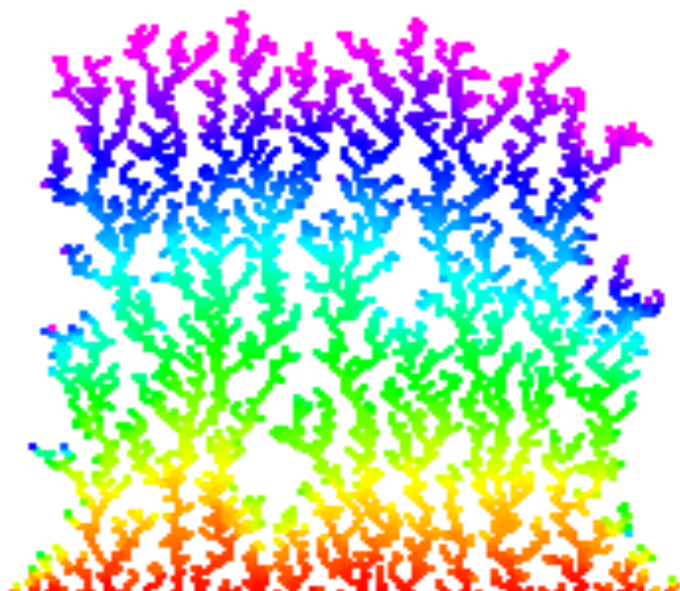
The the Kernel of the Euclidean response defines the Laplace transform

$$K(\tau, \omega) = e^{-\tau\omega}$$

At finite imaginary time the contributions from large energy transfer are quickly suppressed



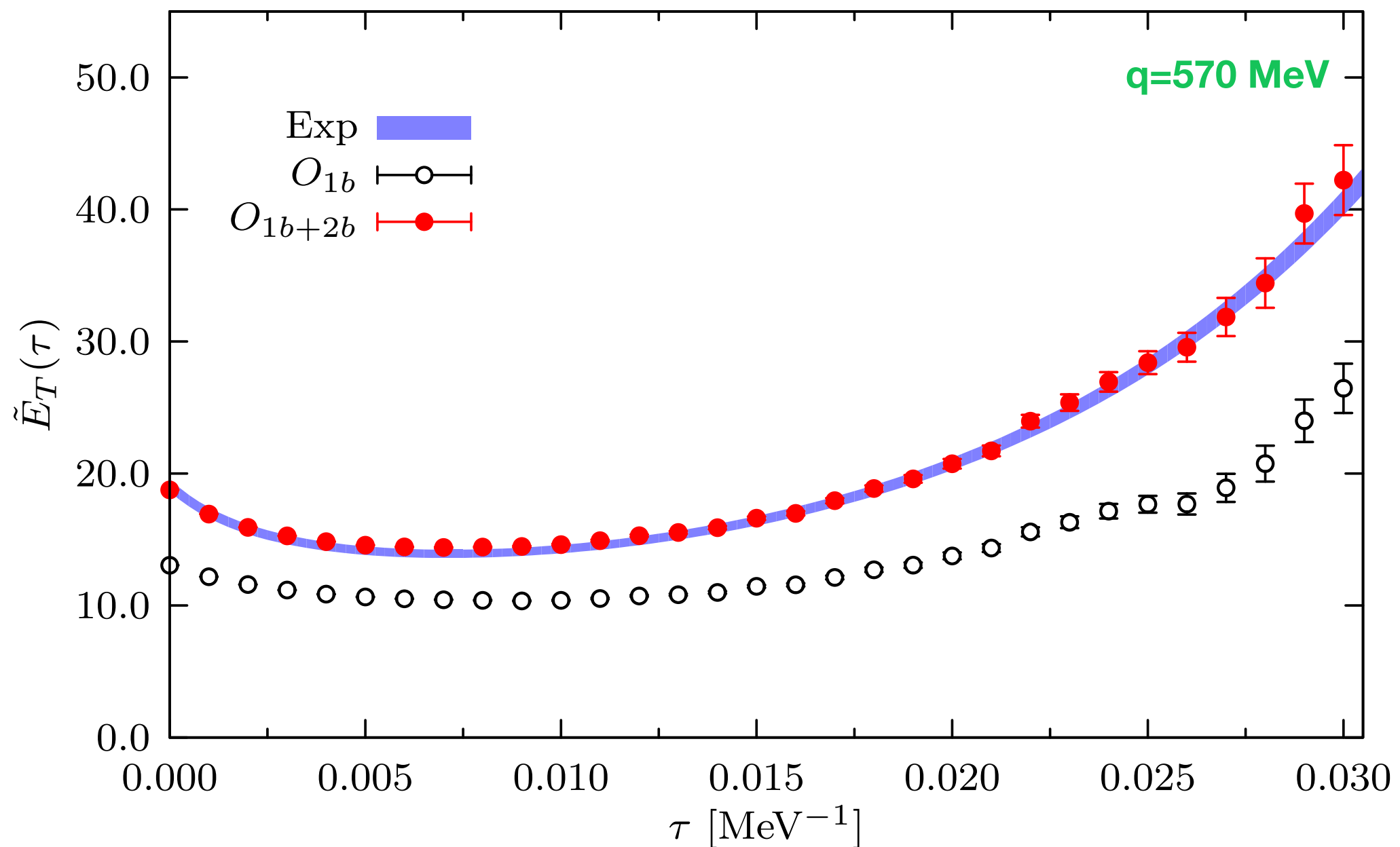
The system is first heated up by the transition operator. How it cools down determines the Euclidean response of the system



$$\frac{\langle \Psi_0 | J_\alpha^\dagger(\mathbf{q}) e^{(H-E_0)\tau} J_\beta(\mathbf{q}) | \Psi_0 \rangle}{\langle \Psi_0 | e^{(H-E_0)\tau} | \Psi_0 \rangle}$$

^{12}C electromagnetic Euclidean response

In the electromagnetic transverse case, two-body current contributions substantially increase the one-body response. This enhancement is effective over the whole imaginary-time region we have considered.



Inversion of the Euclidean response

The Euclidean response formalism allows one to extract dynamical properties of the system from its ground-state.

- Best suited for quantum Monte Carlo approaches
- Wide range of applicability: atomic physics, cold atoms, neutrino scattering, neutron star cooling...

Inverting the Euclidean response is an ill posed problem: any set of observations is limited and noisy and the situation is even worse since the kernel is a smoothing operator.

$$E_{\alpha\beta}(\tau, \mathbf{q}) \longrightarrow R_{\alpha\beta}(\omega, \mathbf{q})$$



We have found **maximum entropy technique** to be best suited for our purposes.

Image reconstruction from incomplete and noisy data

S. F. Gull & G. J. Daniell*

Mullard Radio Astronomy Observatory, Cavendish Laboratory, Madingley Road, Cambridge, UK

Results are presented of a powerful technique for image reconstruction by a maximum entropy method, which is sufficiently fast to be useful for large and complicated images. Although our examples are taken from the fields of radio and X-ray astronomy, the technique is immediately applicable in spectroscopy, electron microscopy, X-ray crystallography, geophysics and virtually any type of optical image processing. Applied to radioastronomical data, the algorithm reveals details not seen by conventional analysis, but which are known to exist.

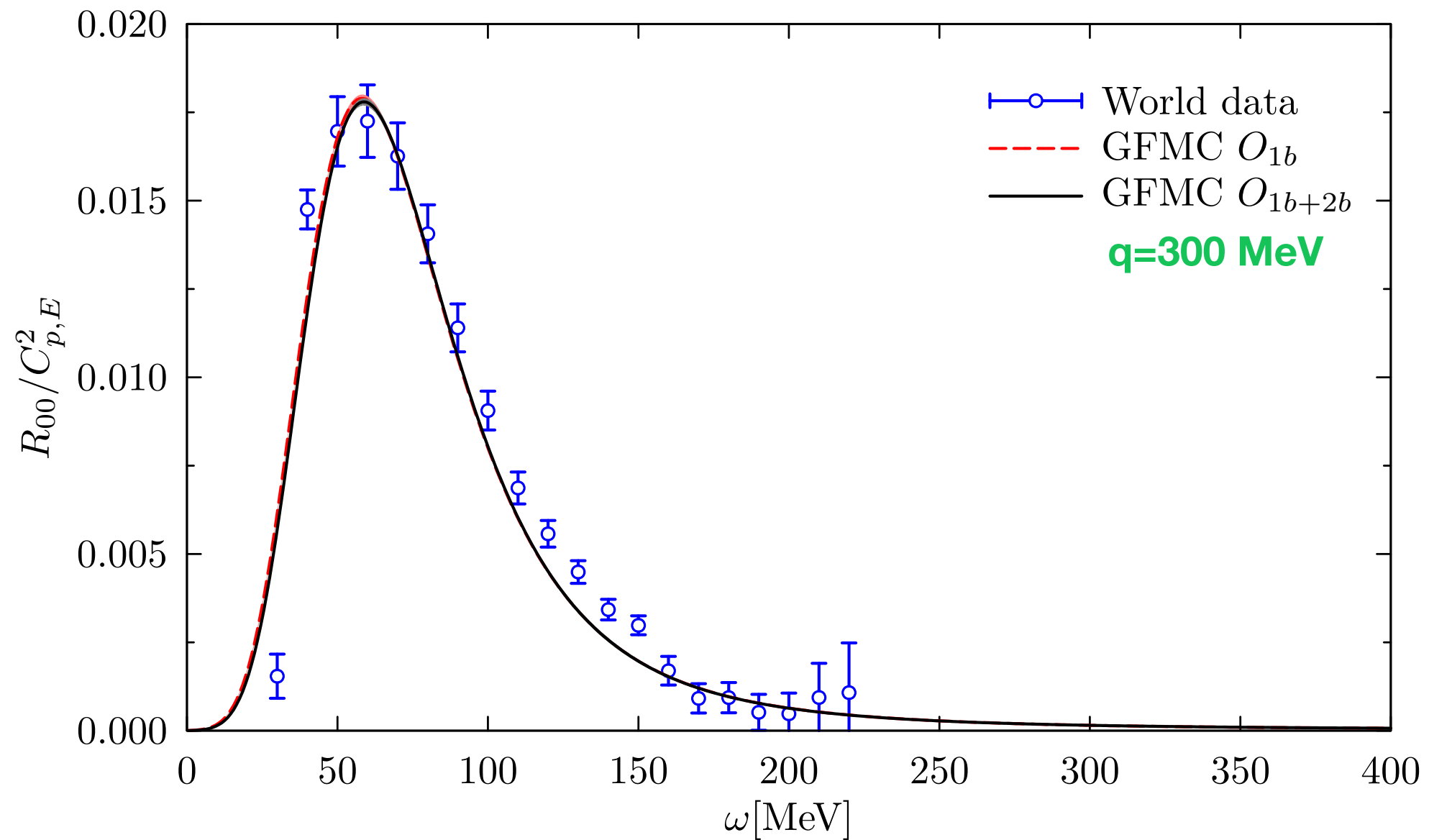
To avoid abstraction, we shall refer to our radioastronomical example. Starting with incomplete and noisy data, one can obtain by the Backus–Gilbert method a series of maps of the distribution of radio brightness across the sky, all of which are consistent with the data, but have different resolutions and noise levels. From the data alone, there is no reason to prefer any one of these maps, and the observer may select the most appropriate one to answer any specific question. Hence, the method cannot produce a unique ‘best’ map of the sky. There is no single map that is equally suitable for discussing both accurate flux measurements and source positions.

Nevertheless, it is useful to have a single general-purpose map of the sky, and the maximum-entropy map described here fulfils

Nature, 272, 688 (1978)

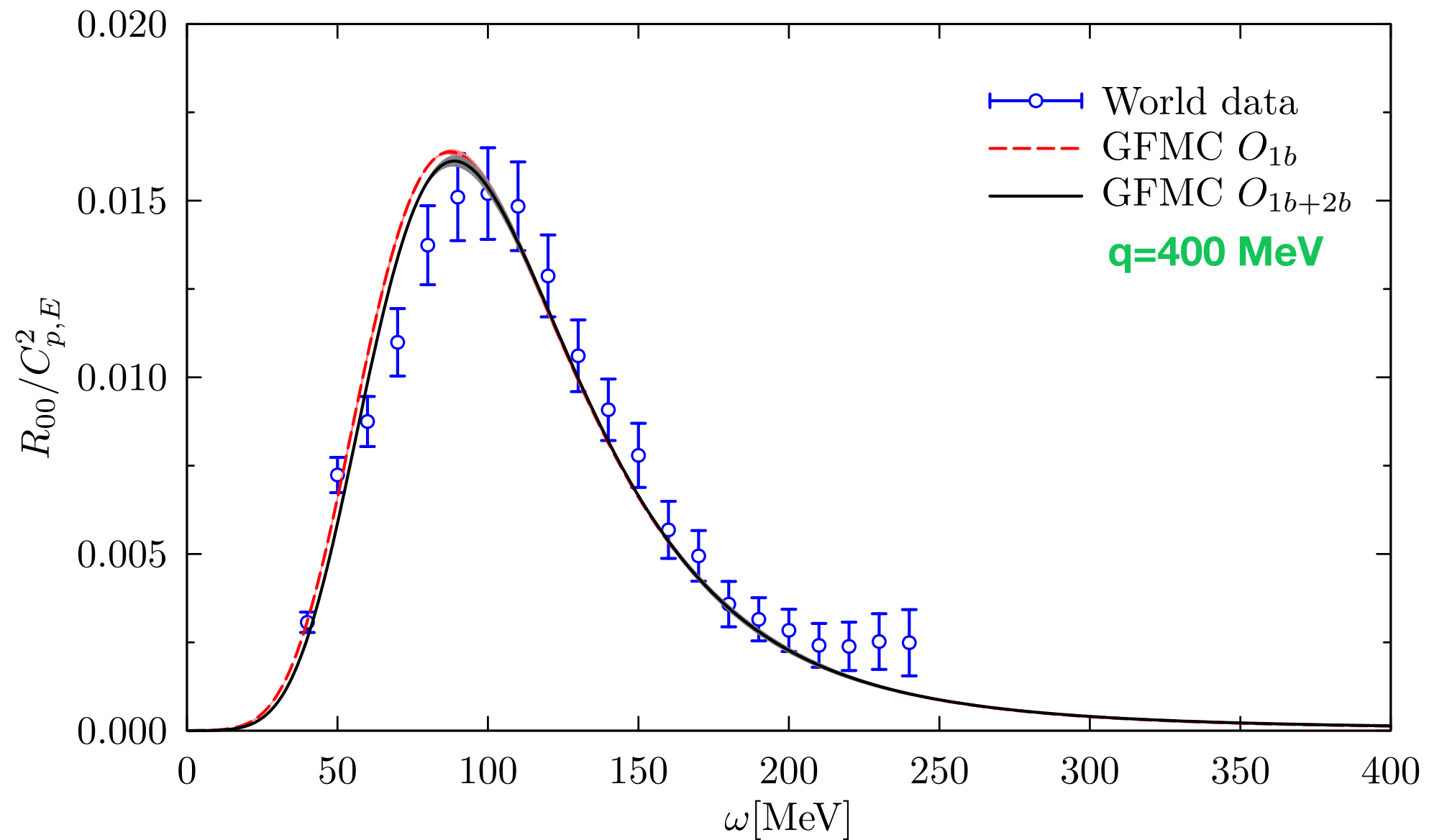
^4He electromagnetic response

Two-body currents do not provide significant changes in the longitudinal response.
The agreement with experimental data appears to be remarkably good.



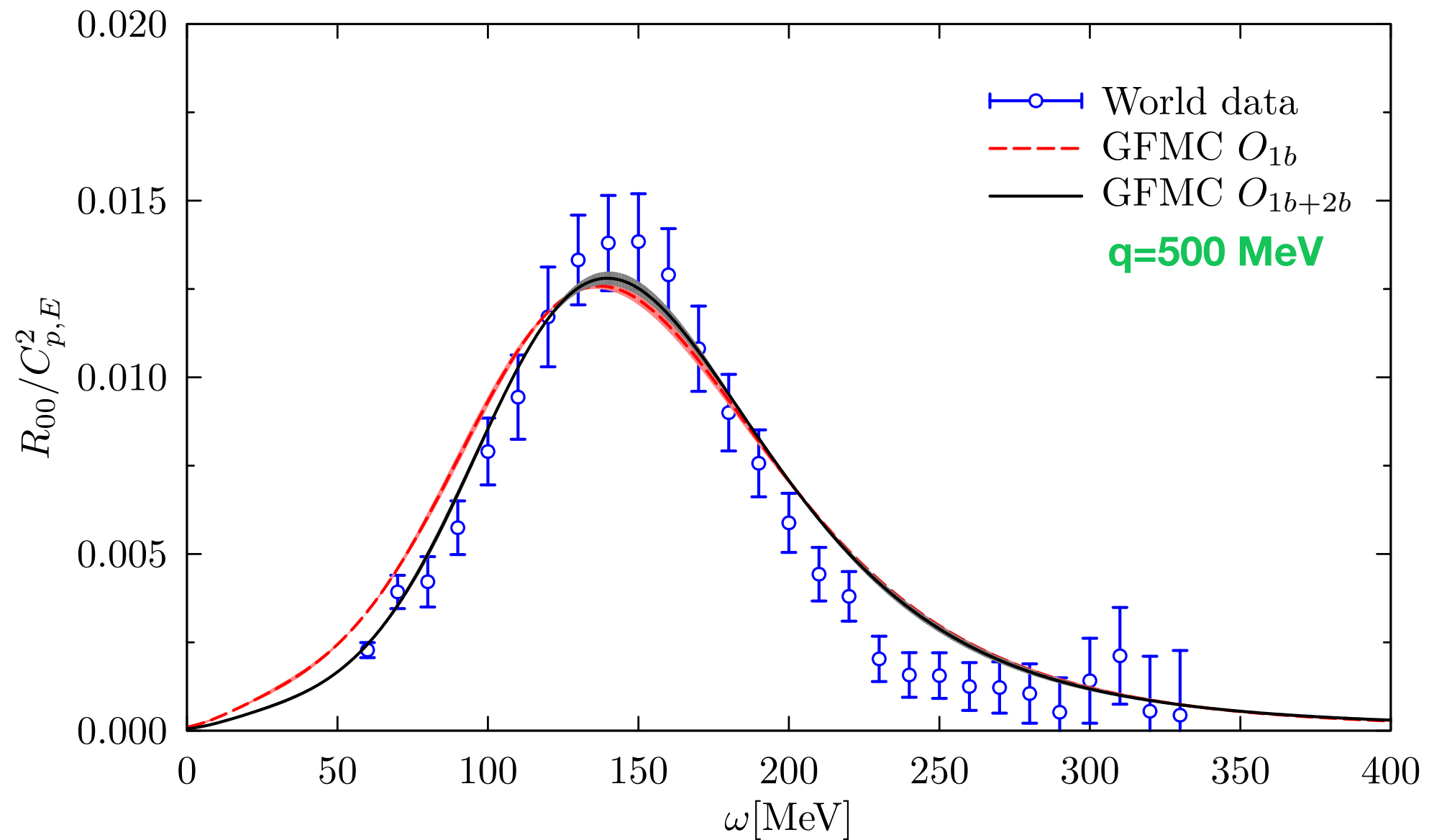
^4He electromagnetic response

Two-body currents do not provide significant changes in the longitudinal response. The agreement with experimental data appears to be remarkably good.



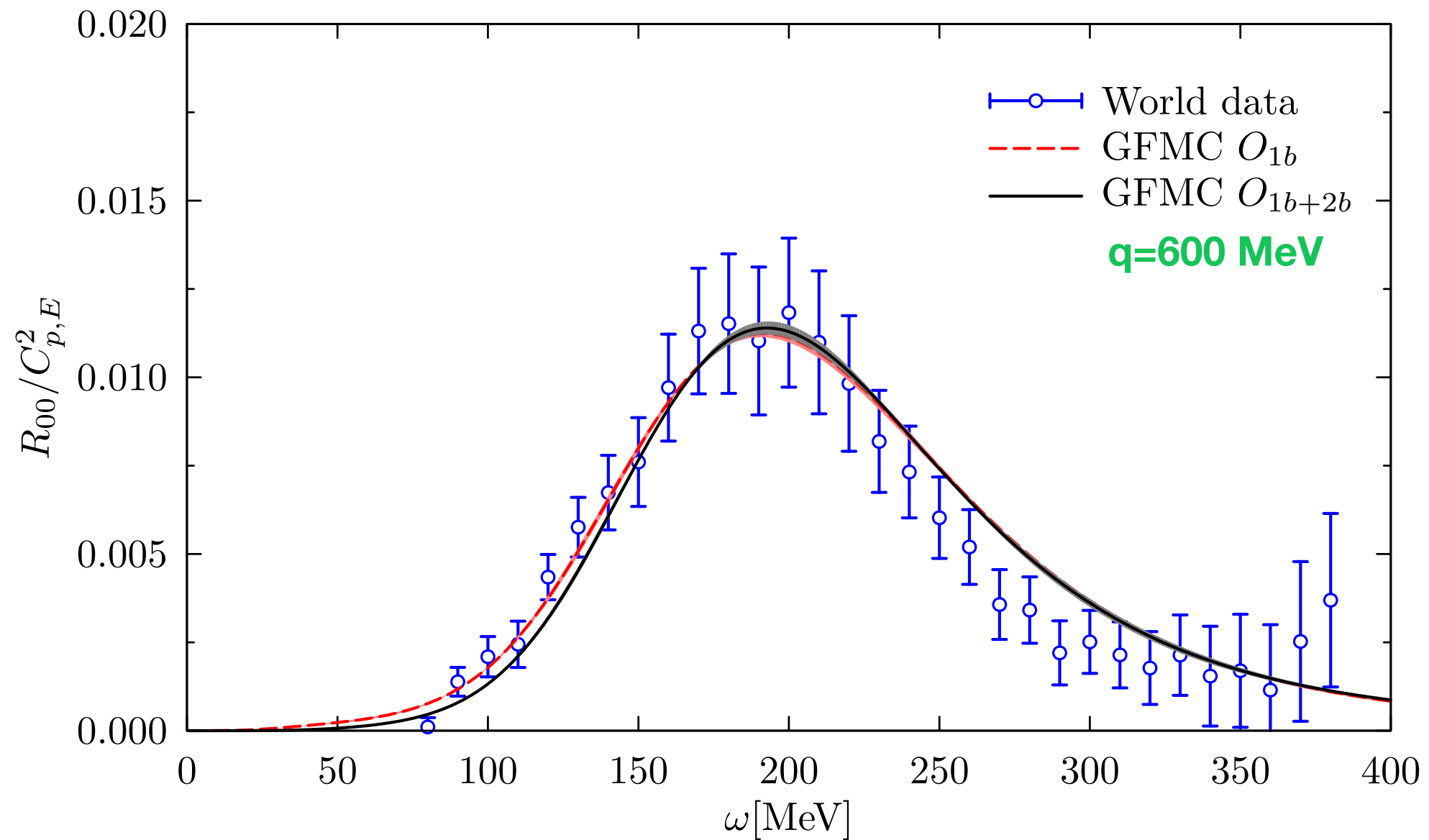
^4He electromagnetic response

Two-body currents do not provide significant changes in the longitudinal response. The agreement with experimental data appears to be remarkably good.



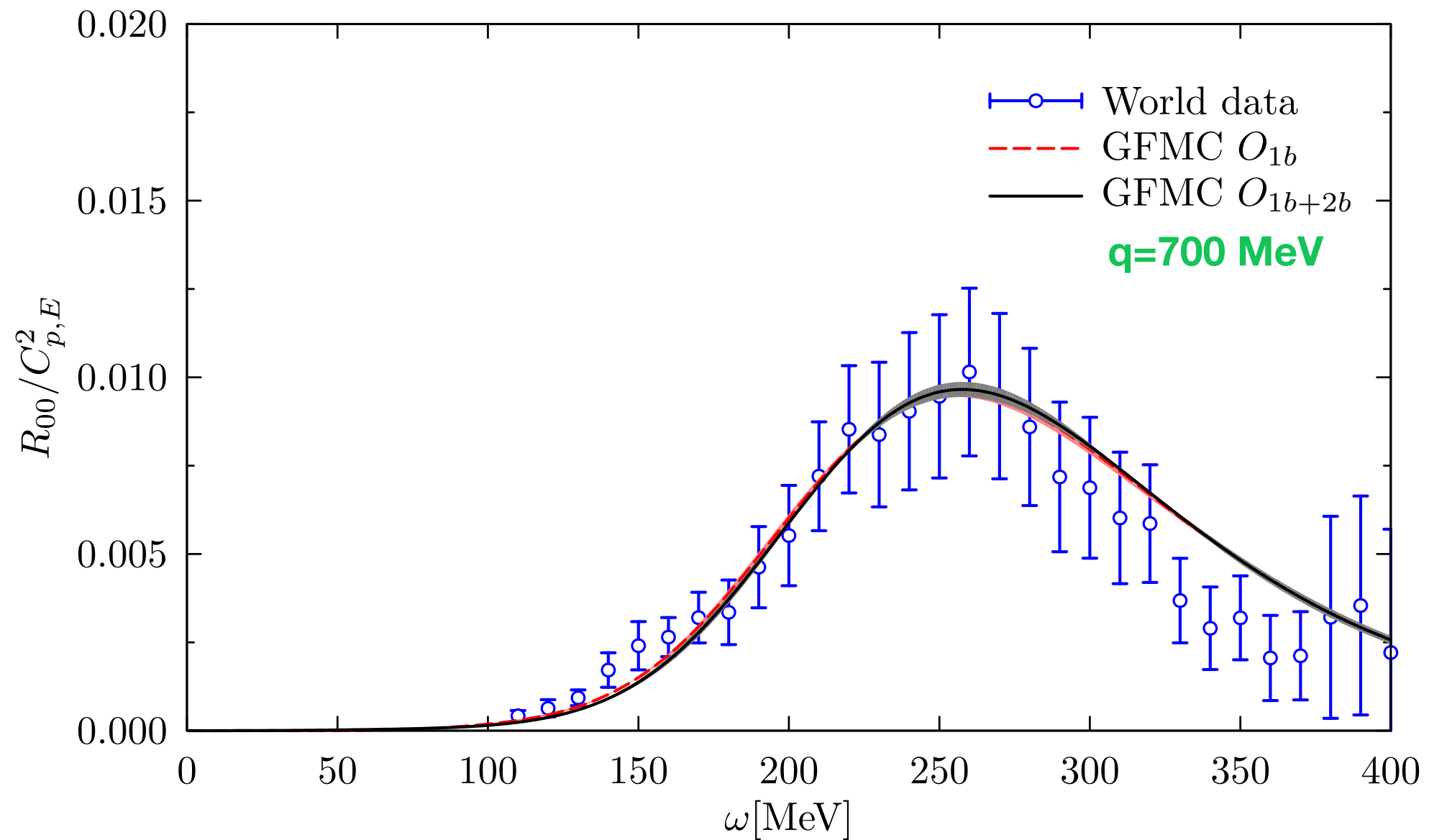
^4He electromagnetic response

Two-body currents do not provide significant changes in the longitudinal response. The agreement with experimental data appears to be remarkably good.



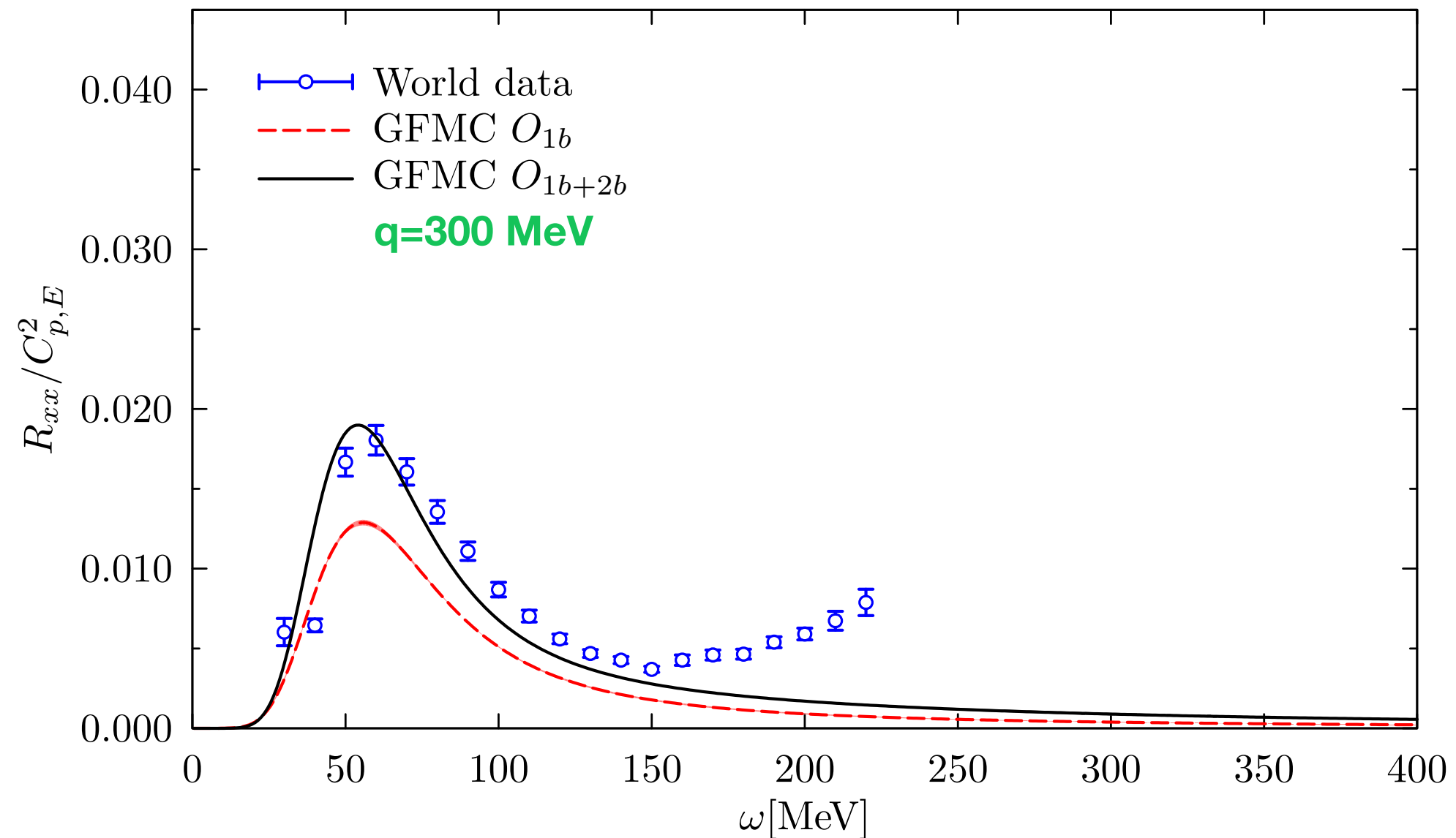
^4He electromagnetic response

Two-body currents do not provide significant changes in the longitudinal response. The agreement with experimental data appears to be remarkably good.



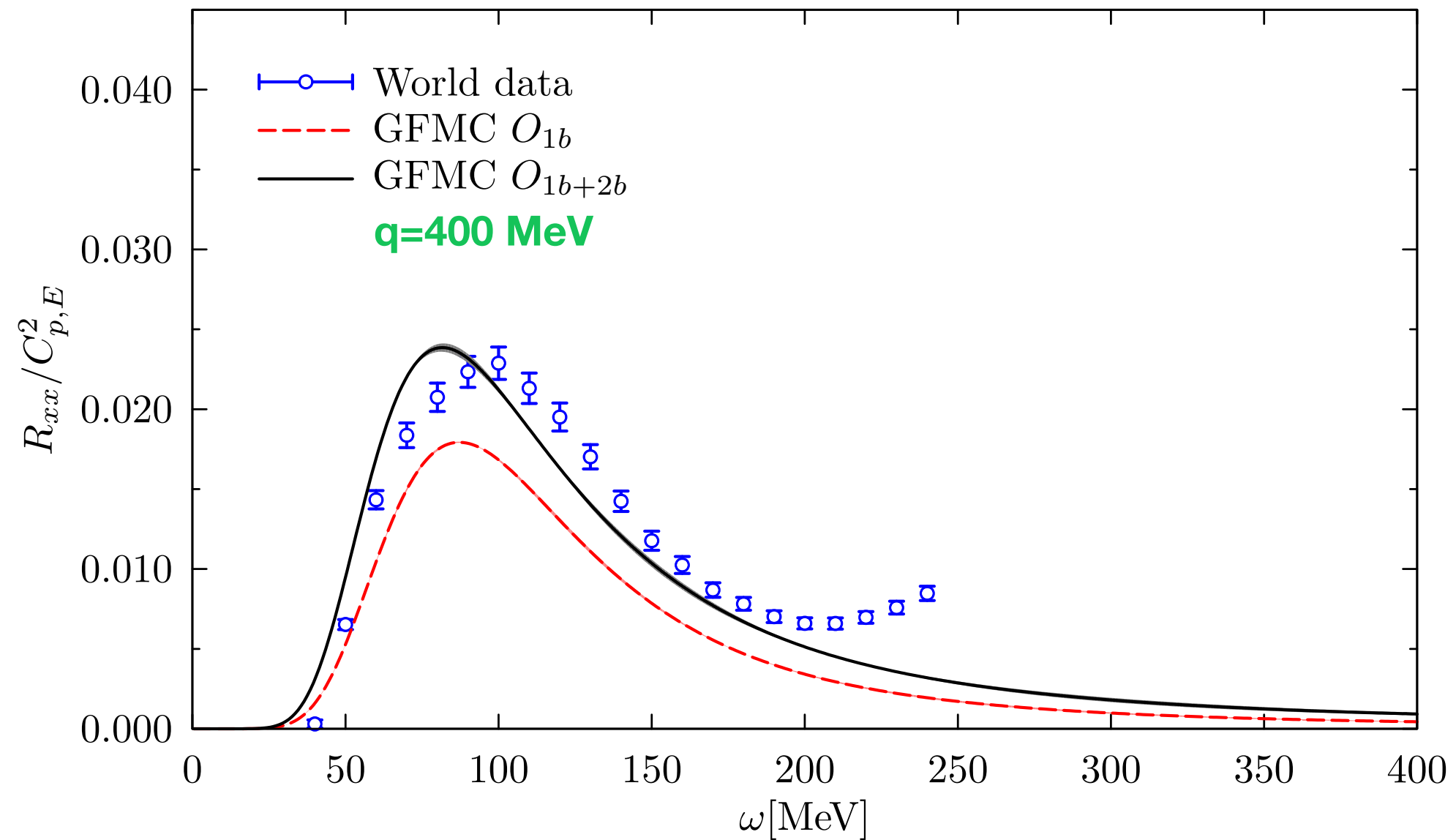
^4He electromagnetic response

Two-body currents significantly enhance the transverse response function, not only in the dip region, but also in the quasielastic peak and threshold regions.



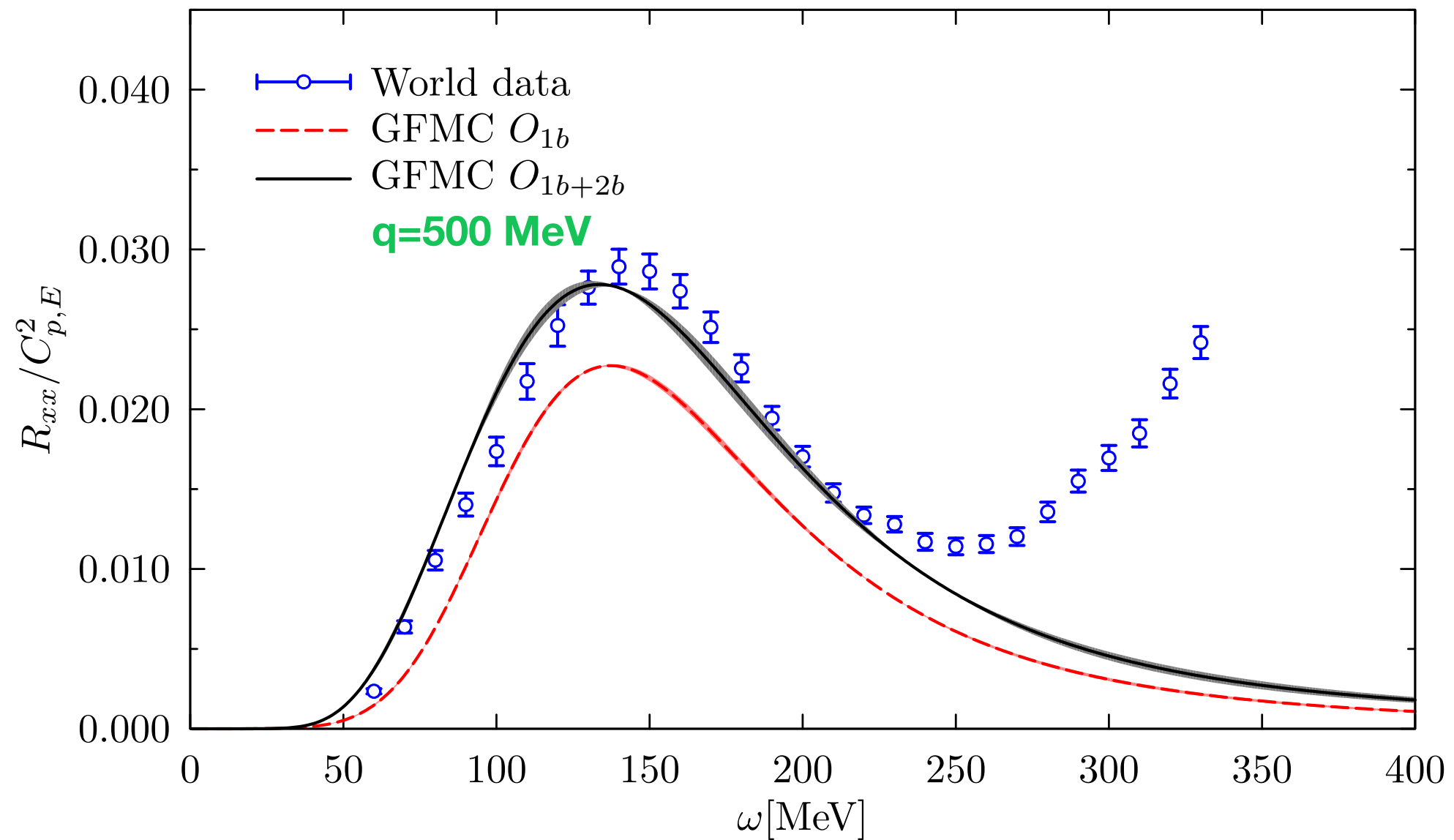
^4He electromagnetic response

Two-body currents significantly enhance the transverse response function, not only in the dip region, but also in the quasielastic peak and threshold regions.



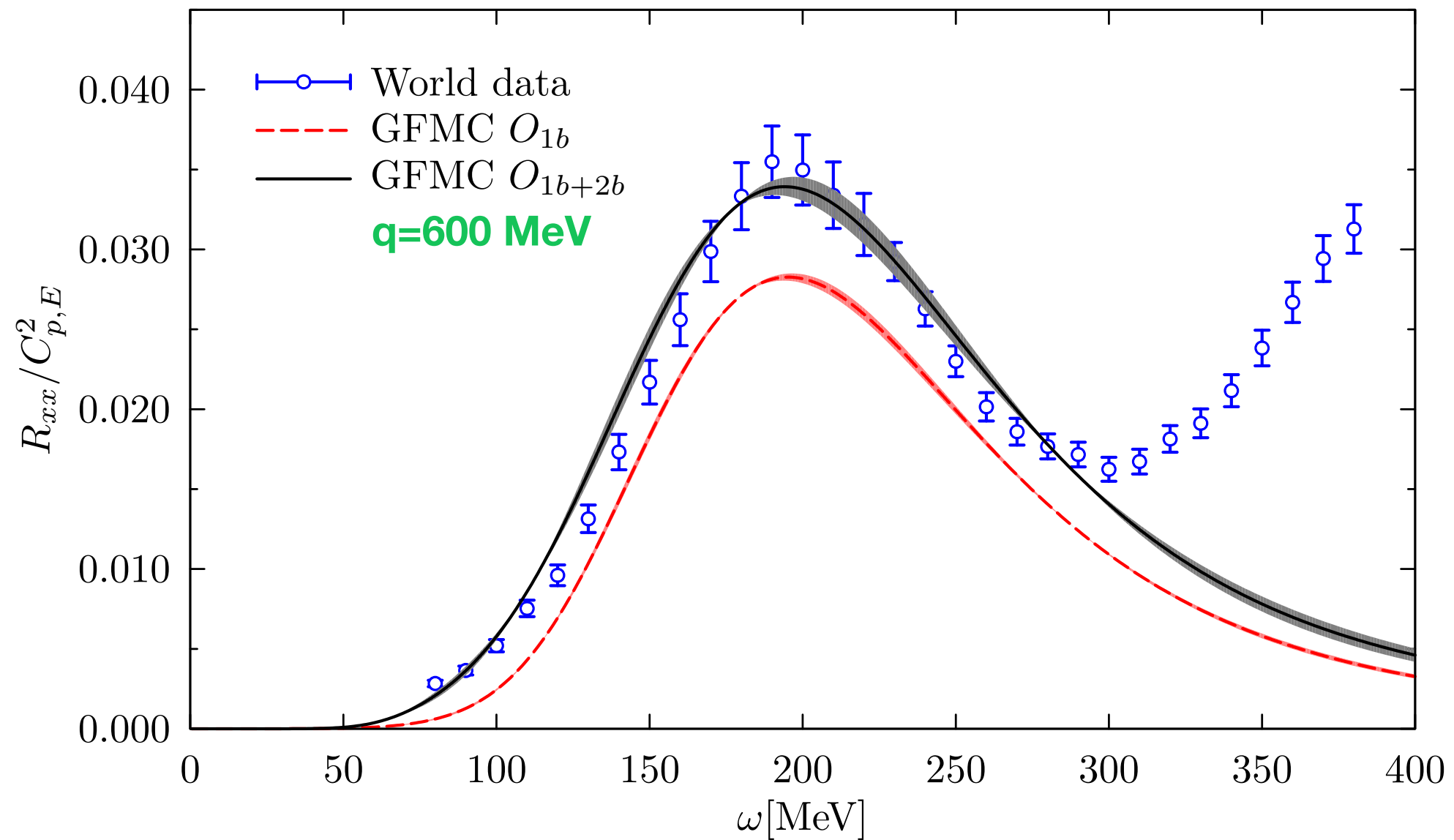
^4He electromagnetic response

Two-body currents significantly enhance the transverse response function, not only in the dip region, but also in the quasielastic peak and threshold regions.



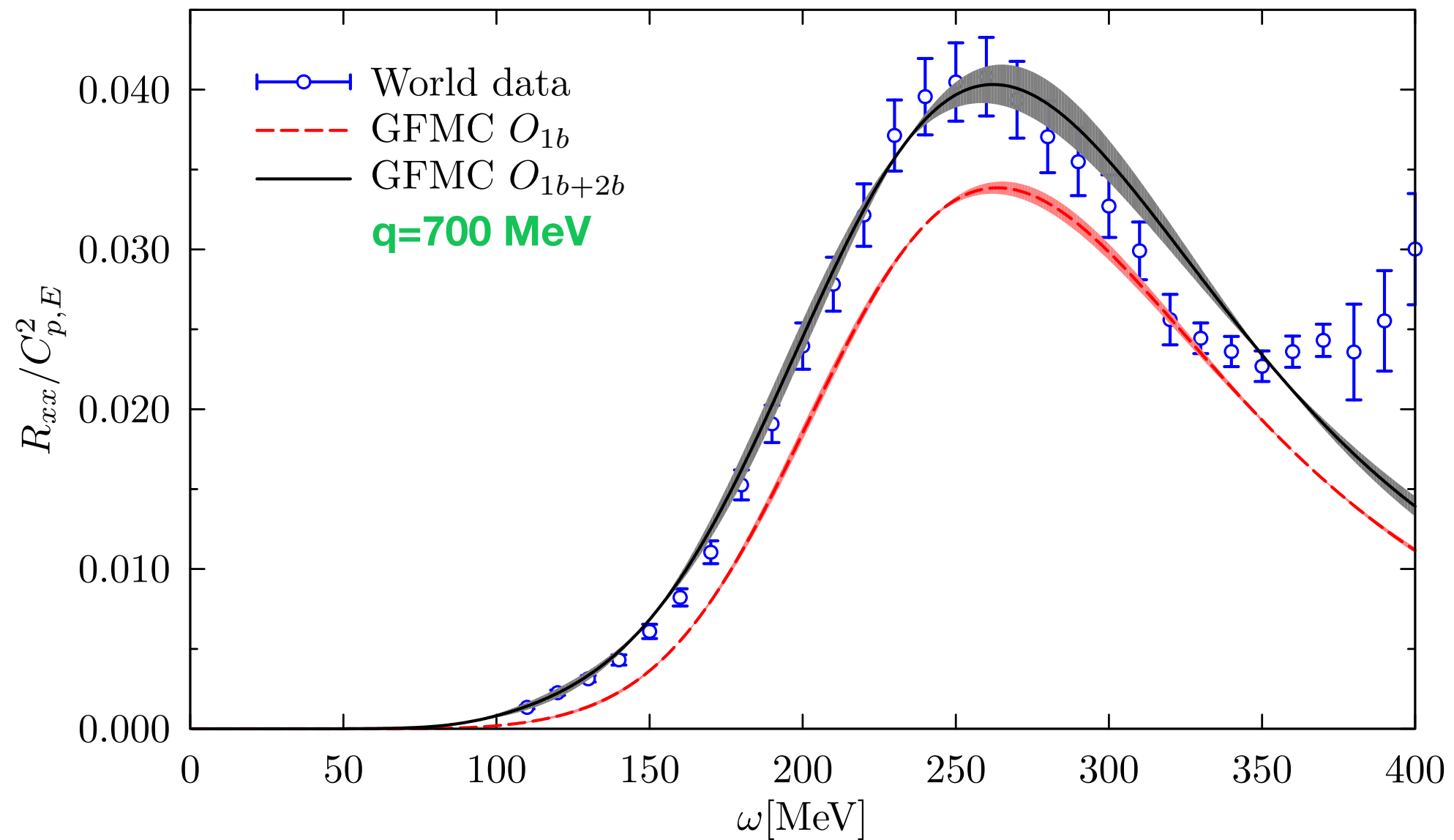
^4He electromagnetic response

Two-body currents significantly enhance the transverse response function, not only in the dip region, but also in the quasielastic peak and threshold regions.



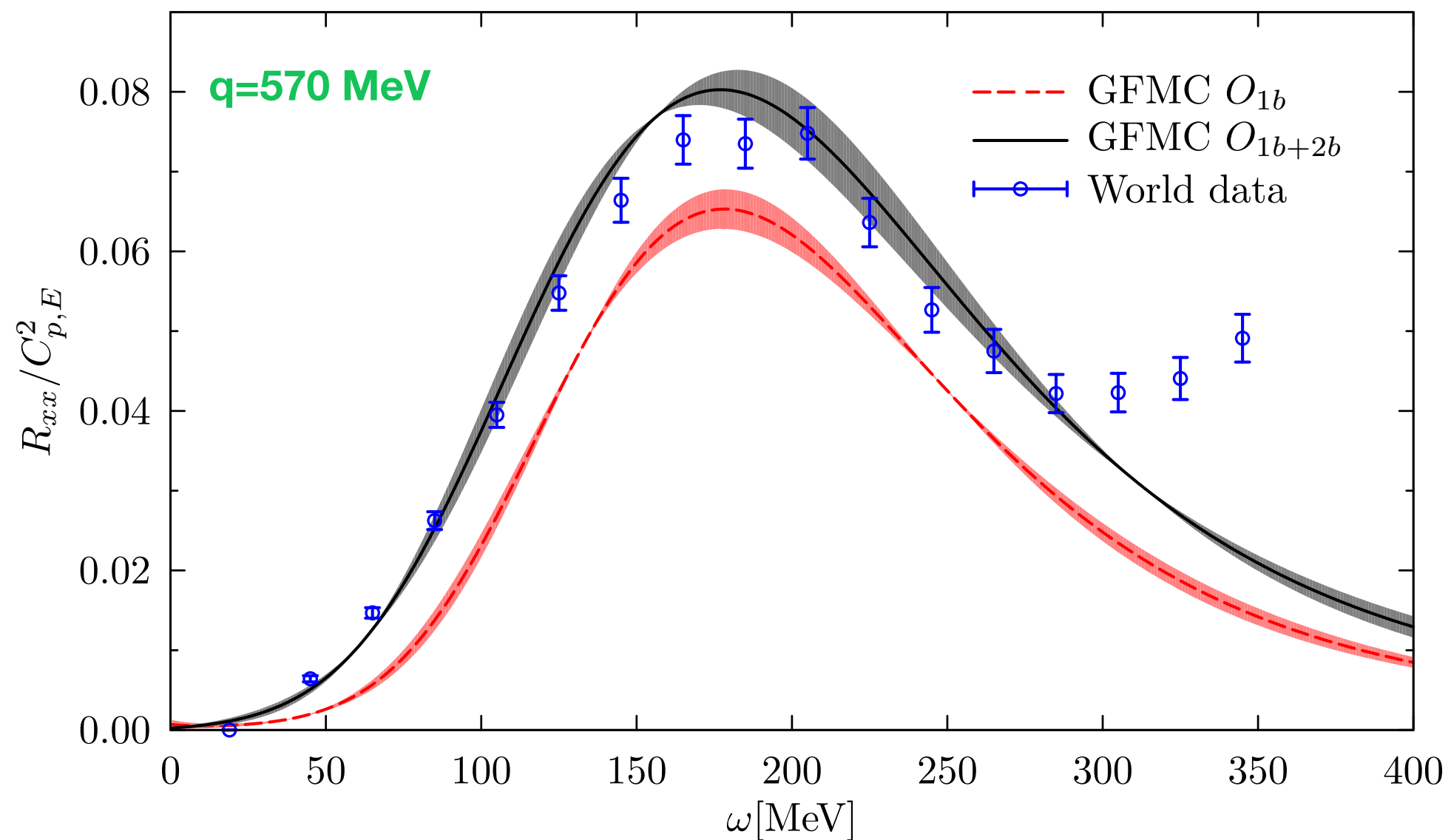
^4He electromagnetic response

Two-body currents significantly enhance the transverse response function, not only in the dip region, but also in the quasielastic peak and threshold regions.



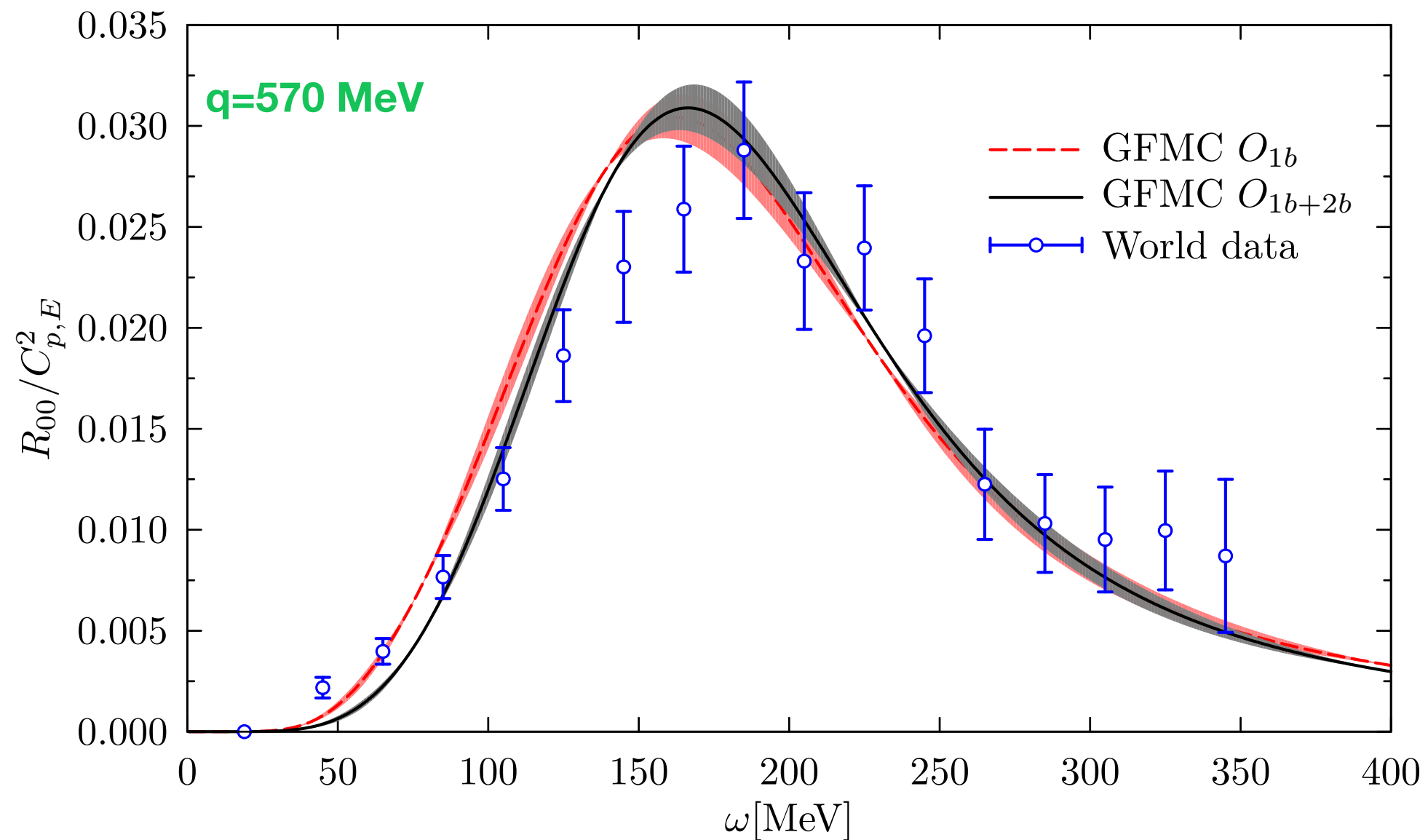
^{12}C electromagnetic response

- Preliminary results on the inversion of the ^{12}C Euclidean response are promising. Need for more statistic (and computing time) and improved inversion techniques.



^{12}C electromagnetic response

- Preliminary results on the inversion of the ^{12}C Euclidean response are promising. Need for more statistic (and computing time) and improved inversion techniques.



This is the end (for now)

Question

Solve the sign problem

The hyperon puzzle

The appearance of hyperons in the inner core of the star strongly depends on the details of the underlying hypernuclear force

- The same hyperon-nucleon potential has been employed in AFDMC calculations to determine the equation of state and the mass-radius relation of an infinite system of neutrons and Λ particles.
- Possibility of a 2 solar masses neutron star: new hints for the solution of the hyperon puzzle.

